Published in final edited form as:
Biochemistry. 2006 October 3; 45(39): 11958–11973.

S. cerevisiae Replication Protein A (scRPA) Binds to Single–stranded DNA in Multiple Salt-dependent Modes†

Sangaralingam Kumaran, **Alexander G. Kozlov**, and **Timothy M. Lohman***
Department of Biochemistry and Molecular Biophysics Washington University School of Medicine 660 S. Euclid Ave. St. Louis, MO 63110

Abstract

We have examined the single stranded DNA binding properties of the *S. cerevisiae* Replication Protein A (scRPA) using fluorescence titrations, isothermal titration calorimetry and sedimentation equilibrium in order to determine whether scRPA can bind to ssDNA in multiple binding modes. We measured the occluded site size for scRPA binding poly(dT), as well as the stoichiometry, equilibrium binding constants and binding enthalpy of scRPA-($(dT)_L$) complexes as a function of oligodeoxynucleotide length, *L*. Sedimentation equilibrium studies show that scRPA is stable hetero-trimer over the range of [NaCl] examined (0.02 M to 1.5 M). However, the occluded site size, *n*, undergoes a salt-dependent transition between values of *n*=18−20 nucleotides at low [NaCl] to *n*=26 −28 nucleotides at high [NaCl], with a transition midpoint near 0.36 M NaCl (25.0°C, pH 8.1). Measurements of the stoichiometry of scRPA-$(dT)_L$ complexes also show a [NaCl]-dependent change in stoichiometry consistent with the observed change in occluded site size. Measurements of the ΔH_{obs} for scRPA binding to $(dT)_L$ at 1.5 M NaCl, yield a contact site size of 28 nucleotides, similar to the occluded site size determined at this [NaCl]. Altogether, these data support a model in which scRPA can bind to ssDNA in at least two binding modes, a low site size mode ($n = 18 \pm 1$ nucleotides), stabilized at low [NaCl], in which only three of its OB-folds are used, and a higher site size mode ($n = 27 \pm 1$ nucleotides), stabilized at higher [NaCl], which uses four of its OB-folds. No evidence for highly cooperative binding of scRPA to ssDNA was found either under any conditions examined. Thus, scRPA shows some similar behavior to the *E. coli* SSB homo-tetramer, which also shows binding mode transitions, but some significant differences also exist.

Single stranded (ss) DNA binding (SSB) proteins exist in nearly all organisms and play central roles in all aspects of DNA metabolism, including DNA replication, repair, and recombination. However, the structural forms of SSB proteins differ considerably among different organisms. For example, the bacteriophage T4 gene 32 protein, the first such SSB protein identified (1, 2) is a monomer, whereas the *E. coli* SSB protein, is a homotetramer (3,4), as are most SSB proteins from eubacteria. In contrast, the eukaryotic SSB protein, commonly called Replication Protein A (RPA) is a hetero-trimer (5,6).

In all eukaryotes, RPA consists of three highly conserved subunits of approximately 70, 32, and 14 kDa, named according to their respective molecular weights, and all three subunits are required for function *in vivo* (5,6). However, RPA homologues display distinct species specificity, such that scRPA from yeast cannot substitute for human RPA (hsRPA) in cell free

†This research was supported in part by the NIH (RO1 GM30498)

*Address correspondence to: Department of Biochemistry and Molecular Biophysics, Box 8231 Washington University School of Medicine 660 South Euclid Ave. St. Louis, M0 63110 E-mail: lohman@biochem.wustl.edu Tel: (314)-362−4393 FAX: (314)-362−7183.

SUPPORTING INFORMATION AVAILABLE Figure showing the results of agarose gel electrophoresis experiments at low (20 mM) and high (1.5 M) NaCl concentrations for scRPA-ssDNA complexes formed at different protein to DNA ratios indicating low or no cooperativity upon formation of these complexes. This material is available free of charge via the internet at http://pubs.acs.org.

SV40 replication assays (7,8). These specificities presumably reflect the fact that RPA proteins also are involved in myriad interactions with other proteins. These include, DNA polymerase α (9), XPA (10), XPG (11), XPF-ERCCI (12), proteins in the Rad52 epistasis group (13), and the Blooms (14) and Werner helicases (15), as well as many others (16-19).

Although SSB proteins from different organisms can differ in architecture, one common feature is that the sites for ssDNA binding consist primarily of so-called oligosaccharide/ oligonucleotide binding folds (OB-folds) (20). Whereas T4 gene 32 protein contains one OB-fold, the *E. coli* SSB tetramer contains four OB-folds and the hetero-trimeric RPA contains six OB-folds. Each OB-fold within RPA could potentially provide a site for ssDNA binding (21-24). Four OB-folds are located within RPA70, referred to as F, A, B and C, (see Figure 1), a fifth OB-fold (D) is contained within the RPA32 subunit, and a sixth OB-fold (E) is contained within RPA14.

The ssDNA binding properties of RPA have previously been characterized using a variety of approaches (25-29). As is true for most SSB proteins, RPA binds with high affinity to ssDNA with no apparent sequence specificity (26,29-32), although it does display a preference for polypyrimidines (26). The primary sites on RPA that interact with ssDNA have been mapped to the central part of the RPA70 subunit (OB-folds A and B) (21,33-35), whereas the N-terminal OB fold of RPA70 participates in protein-protein interactions (9). There is no evidence that the OB-fold of RPA14 (OB-fold E) has DNA binding activity (36,37). There is also evidence that OB-fold D in RPA32 can interact with ssDNA, although this depends on the length of the ssDNA oligodeoxynucleotide (27) as well as the solution conditions (37).

The *E. coli* SSB tetramer, which contains four OB-folds (one per subunit) can bind to ssDNA using either two subunits in its $(SSB)_{35}$ mode (highly cooperative binding mode with occluded site size of 35 nucleotides) or all four subunits in its $(SSB)_{65}$ mode (low cooperative binding mode with occluded site size of 65 nucleotides) depending on solution conditions (3,4, 38-42), and the transition between these modes depends upon salt concentration and type, temperature and pH (39,43-45). By analogy with *E. coli* SSB, it has been suggested that RPA might also bind in various “binding modes” differing in the number of OB-folds that interact with the ssDNA (37,46). Some support for this proposal has come from mutagenesis studies (27) with short oligodeoxynucleotides; however, there is little evidence suggesting that RPA can bind to long ssDNA in multiple binding modes, or that RPA might undergo transitions among alternative binding modes in solution.

The binding site size of RPA when bound to ssDNA has been measured for RPA from a variety of species, with variable results depending on the approach used, but also the species. There appears to be general agreement for the binding site size of human RPA (hRPA) on ssDNA (30 nucleotides) (25,28), although a less stable mode involving interactions with only 8−10 nucleotides of ssDNA, that is observable only upon cross-linking, has also been reported (28). A site size of 22 nucleotides has been reported for *D. melanogaster* (dm) RPA (32); 20 −25 nucleotides for calf thymus RPA (30) and 20−30 nucleotides for RPA from primates (47). However, the reported site sizes for yeast scRPA binding to ssDNA vary over a much wider range from 20 − 90 nucleotides (29,48,49). Furthermore, there is evidence suggesting that the ssDNA binding properties of hRPA and scRPA differ in detail (48). Finally, there seems to be no consensus on the site sizes that characterize any proposed different binding modes (27,50,51).

One difficulty in assessing whether the range of RPA binding site sizes reported reflect true differences is that these studies used a variety of different approaches and were performed under different solution conditions. Since the *E. coli* SSB tetramer in complex with ssDNA has been shown to undergo a salt dependent binding mode transition (39,52), it is possible that

some of the variability observed for the scRPA binding site size is due to differences in the solution conditions used. We have therefore undertaken a systematic study to examine whether scRPA binds to ssDNA in different binding modes using the same approaches (fluorescence, isothermal titration calorimetry and analytical sedimentation) previously used to examine the *E. coli* SSB protein.

MATERIALS AND METHODS

Reagents and Buffers

All buffers were prepared from reagent grade chemicals using double distilled-water that was further de-ionized using a Milli-Q purification system. (Millipore Corp., Bedford, MA). Buffer T is 10 mM Tris (pH 8.1), 0.1 mM Na_3 EDTA. Filter binding buffer is 30 mM HEPES pH 7.8, 5 mM $MgCl_2$, 100 mM NaCl, 0.5% inositol (w/v), and 1 mM Dithiothreitol.

scRPA Protein and Nucleic Acids

The expression vector (p11d-sctRPA) encoding the genes for all three subunits of scRPA (generous gift from Dr. Marc S. Wold, University of Iowa) was used to transform *E. coli* BL21 (DE3) cells. The scRPA hetero-trimer was expressed and purified as described (48) with the following modification. ScRPA was eluted from the anion exchange column (Mono Q 5/50 GL, Pharmacia) using a 10 mL linear KCl gradient from 100 to 400 mM KCl. ScRPA elutes at ~ 300 mM KCl with a yield of 0.8−1.0 mg/L of culture. We also included a single stranded DNA cellulose column as an additional purification step to be sure that all RPA used in our experiments has ssDNA binding activity. The ssDNA cellulose column was equilibrated with buffer T + 0.3 M NaCl before loading the protein. The protein that eluted from the Mono-Q column was diluted two-fold with buffer T + 0.02 M NaCl before loading onto the ssDNA column. The ssDNA column was washed successively with buffer T + 0.3 M NaCl, buffer T + 0.5 M NaCl, and the ScRPA was eluted with buffer T + 2.0 M NaCl + 10%(v/v) glycerol. The purity of scRPA was >98%, judged by SDS-polyacrylamide gel electrophoresis. The purified protein was dialyzed into buffer T plus 0.1 M NaCl, 0.2 mM 2 mercaptoethanol, and 30%(v/v) glycerol, and stored at −20°C. The scRPA concentration was determined spectrophotometrically in buffer T (0.02 M NaCl) by using an extinction coefficient of 9.85×10^4 M^{-1} cm^{-1} (48).

The oligodeoxynucleotides, $(dT)_L$, were synthesized and purified as described (41) and were ≥ 98% pure as judged by denaturing gel electrophoresis. The 5′-Cy3$(dT)_{29}$ used for sedimentation studies was further purified by reverse phase HPLC using an Xterra MS C18 Column (Waters, Milford, MA). The poly(dT) (Midland certified reagent company, Midland, TX((Catalog #P-2004, Lot number 040495)), had an average length of ~ 1100 (Midland Certified Reagent Company). All DNA samples were dissolved in buffer T and dialyzed extensively before use. Single stranded circular M13 mp18 DNA was purchased from New England Biolabs (Catalog #N4040S; Lot number 11) and was supplied in 10 mM Tris-HCl (pH 7.5), 1 mM EDTA. Concentrations of the nucleic acids were determined spectrophotometrically using the extinction coefficients: $(dT)_L$ and poly(dT): $\varepsilon_{260} = 8.1 \times 10^3$ M^{-1} (nucleotide) cm^{-1} (53); single stranded M13 DNA: $\varepsilon_{259} = 7370$ M^{-1} cm^{-1} (54); Cy3-(dT) $\varepsilon_{260} = 2.6 \times 10^5$ M^{-1} cm^{-1}, calculated as described (55).

Analytical ultracentrifugation

Sedimentation equilibrium and velocity experiments were performed using an Optima XL-A analytical ultracentrifuge and an An50Ti rotor (Beckman Instruments, Inc., Fullerton, CA). All samples were dialyzed extensively versus buffer T containing the indicated amount of salt. Sedimentation equilibrium experiments were performed at three different protein concentrations (120 μl) using an Epon charcoal-filled six channel centerpiece. Experiments

were also usually performed at three rotor speeds starting with the slowest rotor speed. Samples were scanned at a wavelength of 280 nm and data were collected at a spacing 0.001 cm with an average of 7 scans per step. Attainment of equilibrium was judged by overlaying at least three successive scans taken at 2-hour intervals. Data sets were edited with WinREEDIT (http://www.biotech.uconn.edu/auf/) to extract the data between the meniscus and the bottom of the cell and were then analyzed by non-linear least squares (NLLS) methods using WINNONLIN (David Yphantis, University of Connecticut; Michael Johnson, University of Virginia; Jeff Lary, National Analytical Ultracentrifuge center, Storrs, CT) and SCIENTIST (Micromath, St. Louis, MO).

Apparent molecular weights were obtained by fitting the sedimentation equilibrium data to equation:

$$A_T = \sum_{i=1}^{n} \exp\left(\ln A_{0,i} + \sigma_i \left(r^2 - r_{ref}^2\right)/2\right) + b \quad (1)$$

where A_T is the total absorbance at radial position r; $A_{0,i}$ is the absorbance of component *i* at reference radial position (r_{ref}); *b* is the baseline offset, $\sigma_i = \left[M_i\left(1 - \bar{\upsilon}_i\rho\right)\omega^2\right]/RT$, M_i is the molecular mass of *i* component, $\bar{\upsilon}_i$ is the partial specific volume of component *i*, ρ is the solution density (calculated using SEDNTREP (David Hayes, Magdalen College; Tom Laue, University of New Hampshire; John Philo, Amgen)), ω is the angular velocity; *R* is the ideal gas constant and *T* is absolute temperature. A global NLLS fit of the absorbance profiles to eq 1 returns *M* for each component present at equilibrium, providing $\bar{\upsilon}_i$ is known. For scRPA, $\bar{\upsilon}_i$ was calculated from its amino acid composition using the program SEDNTREP, yielding 0.7294 ml g^{-1} at 25°C; $\bar{\upsilon}_i$ for Cy3-dT(pT)$_{29}$ was 0.58 (56). Sedimentation equilibrium experiments performed at three different protein concentrations, in buffer T + 200 mM NaCl + 10% (v/v) glycerol were fit to eq 1 using $\bar{\upsilon}_i$ value of 0.7294 ml g^{-1} and values are listed in table 1. The calculated values of $\bar{\upsilon}_i$ were corrected for the presence of 10% (v/v) glycerol as described (57). The corrected value of $\bar{\upsilon}_i$ is 0.7327 (± 0.0016) ml g^{-1}. Cy3-(dT)$_{29}$ alone in buffer T sediments as a single species with M_{app} = 9.8 (± 0.2) kDa, close to the expected value of 9.3 kDa. For the NLLS analysis of protein-DNA complexes, σ_{DNA} was fixed to the value determined independently for DNA, while floating for $\sigma_{protein\text{-}DNA}$ complexes. The values of $\bar{\upsilon}$ for the protein-DNA complexes were calculated as the weight-average sum of $\bar{\upsilon}$ for the individual components, as in equation :

$$\bar{\upsilon}_{RnD} = \frac{nM_{Rf}\,\bar{\upsilon}_{Rf} + M_{Df}\,\bar{\upsilon}_{Df}}{nM_{Rf} + M_{Df}} \quad (2)$$

where $\bar{\upsilon}_{RnD}$ is the partial specific volume for the protein-DNA complex, M_{Rf} and M_{Df} are molecular masses of scRPA and the DNA substrate (g mol^{-1}), and $\bar{\upsilon}_{Rf}$ and $\bar{\upsilon}_{Df}$ are the partial specific volumes of the scRPA and DNA substrate respectively (ml g^{-1}). The sedimentation velocity experiments were analyzed using the program DCDT$^+$ (version 1.16, John S. Philo) to obtain estimates of the molecular masses.

Fluorescence Measurements

Titrations of scRPA with ssDNA were performed by monitoring the intrinsic tryptophan fluorescence of scRPA using a PTI QM-4 spectrofluorometer (Photon Technology International, Lawrenceville, NJ) equipped with a 75 W Xe lamp. The excitation wavelength was 295 nm, and the fluorescence intensity was monitored at 345 nm. All slit widths were set to 0.5 mm and photobleaching under these conditions was less than 2%. The sample temperature was controlled at 25.0 ± 0.2° C using a Lauda RM6 recirculation water-bath

(Brinkmann, Westbury, NY). A 1.9 ml solution of scRPA in a 4.0 ml quartz cuvette (10 mm path length-3 ml) (NSG Precision Cells Inc., Farmingdale, NY) was equilibrated with constant stirring using an 8 mm diameter cylindrical cell stirrer (P-73 from NSG Precision cells, Inc.) for at least 30 minutes until the tryptophan fluorescence intensity reached a constant value. Initial readings of both the sample, $F_{samp,0}$ and reference cuvettes (containing only buffer), $F_{ref,0}$ were then taken, with $F_0 = F_{samp,0} - F_{ref,0}$, defined as the initial fluorescence of the sample. The sample cuvette was then titrated with aliquots of DNA and the solution was equilibrated for 3 minutes with stirring. For each point in the titration, the sample was excited for 10 s during which five data points were taken, after which the shutter was closed. Data points from two such measurements were averaged to obtain $F_{samp,i}$, the fluorescence intensity after the i th addition of DNA. A second cuvette containing buffer was also titrated with DNA yielding the background fluorescence, $F_{ref,i}$. The difference between these two readings is defined as the observed fluorescence for each titration point i, $F_{obs,i}$ (= $F_{samp,i} - F_{ref,i}$). The relative fluorescence quenching upon DNA binding is defined as $Q_{obs,i}=\frac{(F_0 - F_{obs,i})}{F_0}$. All measurements were corrected for dilution, and inner filter effects as described (58).

Model-Independent determination of binding isotherms and stoichiometries of scRPA-ssDNA complexes

The binding of oligodeoxythymidylates, $(dT)_L$, to scRPA was monitored by the quenching of intrinsic tryptophan fluorescence of the protein, Q_{obs}. Model-independent estimates of the average number of moles of $(dT)_L$ bound per mole of scRPA hetero- trimer, $\sum \Theta_i$, were obtained using the Binding Density Function method (59). The observed fluorescence quenching of the scRPA protein at any point in the titration is related to $\sum \Theta_i$ by equation:

$$Q_{obs} = \sum \Theta_i Q_{i_{max}} \tag{3}$$

where $Q_{i_{max}}$ is the extent of fluorescence quenching when a $(dT)_L$ is bound to site i. Since each $Q_{i_{max}}$ is constant for a given state i, then at equilibrium, Q_{obs} is dependent only upon the distribution of $(dT)_L$ bound. Therefore, at any constant value of Q_{obs}, the values of $\sum \Theta_i$ is also constant. Hence, from titrations (Q_{obs} *versus* log D_{tot}) performed at 2 (or more) different concentrations of scRPA protein, $R_{tot,1}$ and $R_{tot,2}$, one can determine the set of values of the concentrations of total nucleic acid, $D_{tot,1}$ and $D_{tot,2}$, for which Q_{obs} is constant, and thus $\sum \Theta_i$ can be calculated from equation:

$$\sum \Theta_i = \frac{D_{tot,2} - D_{tot,1}}{R_{tot,2} - R_{tot,1}} \tag{4}$$

Analysis of fluorescence titrations for the binding of short $(dT)_L$ ($L \leq n$) to one scRPA molecule

Binding of $(dT)_L$ to scRPA with L=20,22,26,28 (1.5 M NaCl) was analyzed to obtain the equilibrium binding constant, $K_{obs}=\frac{[RD]}{[R]\cdot[D]}$, using a single site binding model equation:

$$\frac{Q_{obs}}{Q_{max}} = \frac{K_{L,obs} D}{1 + K_{L,obs} D} \tag{5}$$

where Q_{obs} is observed fluorescence quenching and Q_{max} is the maximum fluorescence quenching observed at saturation of the scRPA (R) with $(dT)_L$ (D) to form RD; D can be found from the mass conservation equation:

$$D_{tot} = D + D_{bound} = D + \frac{K_{L,obs} D}{1 + K_{L,obs} D} R_{tot} \tag{5a}$$

The binding of two $(dT)_{18}$ molecules to scRPA at high salt concentration was analyzed using a two site binding model described in equation:

$$Q_{obs}=\frac{Q_{1,obs}K_{1,obs}D+Q_{2,obs}K_{1,obs}K_{2,obs}D^2}{1+K_{1,obs}D+K_{1,obs}K_{2,obs}D^2} \quad (6)$$

where Q_{obs} is the observed fluorescence quenching and Q_1 and Q_2 are the fluorescence quenchings corresponding to one and two $(dT)_L$ bound, respectively; $K_{1,obs}$ and $K_{2,obs}$ are the step-wise association constants for the binding of the first and the second DNA molecule ($K_{1,obs}=\frac{[RD]}{[R]\cdot[D]}$ and $K_{2,obs}=\frac{[RD_2]}{[RD]\cdot[D]}$); the concentration of free DNA, D, was determined from the mass conservation equation:

$$D_{tot}=D+D_{bound}=D+\frac{K_{1,obs}D+2K_{1,obs}K_{2,obs}D^2}{1+K_{1,obs}D+K_{1,obs}K_{2,obs}D^2}R_{tot} \quad (6a)$$

Fitting of the data to the models in eq 5 and eq 6 was performed using SCIENTIST (Micromath, St Louis, MO)..

Isothermal Titration Calorimetry

ITC experiments were performed in buffer T (25°C) at three [NaCl] (0.02M, 0.2M and 1.5 M), using a VP-ITC calorimeter (Microcal, Northampton, MA) as described (60). Both the scRPA (R) and $(dT)_L$ (D) were dialyzed extensively versus reaction buffer. All samples and buffer solutions were degassed at room temperature prior to use. Most experiments were carried out by titrating scRPA (0.25−1.0 μM) with $(dT)_L$ (5−15 μM), although one experiment at 0.2M NaCl was performed by titrating $(dT)_L$ (0.43 μM) with scRPA (21.1μM). Control experiments to determine the heat of dilution for each injection were performed by injecting the same volumes of $(dT)_L$ (or scRPA) into the sample cell containing only buffer.

The data obtained in 1.5 M NaCl (see Figure 4A and Figure 8) were analyzed using a 1:1 binding model described by equation:

$$Q_i^{tot}=V_0\Delta H\cdot R_{tot}\frac{K_{obs}D}{1+K_{obs}D} \quad (7)$$

where Q_i^{tot} is total heat after i^{th} injection, V_0 is the volume of calorimetric cell, K_{obs} and ΔH are the observed equilibrium binding constant $\left(K_{obs}=\frac{[RD]}{[R]\cdot[D]}\right)$ and corresponding enthalpy change; the concentration of free $(dT)_L$, D, was obtained from equation:

$$D_{tot}=D+D_{bound}=D+R_{tot}\frac{K_{obs}D}{1+K_{obs}D} \quad (7a)$$

In eq 7 and eq 7a, D_{tot} and R_{tot} are the total concentrations of the ssDNA and scRPA in the calorimetric cell after the i^{th} injection. To obtain the binding parameters K_{obs} and ΔH, the experimental data were fit to this model using software provided by the instrument manufacturer. The details of the conversion of integral heats (Q_i^{tot}) to differential heats (heats per injection observed in the experiment) and the fitting routine including corrections for heat displacement effects and DNA and protein dilutions in the cell are described in the “ITC Data Analysis in Origin” Tutorial Guide (Microcal. Inc) and (60).

At 0.02M and 0.2M NaCl, a single $(dT)_{30}$ molecule can bind two molecules of scRPA (see Figure 4B,C,D). Equilibrium binding under these conditions was analyzed using a two-site sequential model, such that the total heat (Q_i^{tot}) after the i^{th} injection is defined by equation:

$$Q_i^{tot} = V_0 D_{tot} \frac{\Delta H_1 \cdot K_{1,obs} R + (\Delta H_1 + \Delta H_2) \cdot K_{1,obs} K_{2,obs} R^2}{1 + K_{1,obs} R + K_{1,obs} K_{2,obs} R^2} \quad (8)$$

where $K_{1,obs}$, ΔH_1 and $K_{2,obs}$, ΔH_2 are the observed step-wise macroscopic equilibrium constants ($K_{1,obs} = \frac{[DR]}{[D] \cdot [R]}$ and $K_{2,obs} = \frac{[DR_2]}{[DR] \cdot [R]}$) and enthalpy changes for binding of the first and second molecule of scRPA to $(dT)_{30}$, respectively; R is the free scRPA concentration, which can be found using equation:

$$R_{tot} = R + R_{bound} = R + D_{tot} \frac{K_{1,obs} R + 2 \cdot K_{1,obs} K_{2,obs} R^2}{1 + K_{1,obs} R + K_{1,obs} K_{2,obs} R^2} \quad (8a)$$

The binding parameters, $K_{1,obs}$, ΔH_1 and $K_{2,obs}$, ΔH_2, were obtained by fitting the experimental data to this model using software provided by the instrument manufacturer as described in the "ITC Data Analysis in Origin" Tutorial Guide (Microcal. Inc) and Kozlov and Lohman, 1998, (60).

Agarose gel electrophoresis

Agarose gel electrophoresis to examine the cooperativity of scRPA-ssM13 DNA complexes was performed as described (61) using 0.5% agarose gels (14 cm horizontal gels). The total reaction volume of each sample was 30 μl. In a series of experiments, the DNA concentration was held constant (0.5 μg), while varying the scRPA concentration. The solution conditions used are given in the text for each experiment. The gel electrophoresis running buffer was 20 mM-Tris (pH 7.8), 0.4 mM-sodiumacetate, 0.2 mM Na_3EDTA. Loading dye (2 μl of 50% (v/v) glycerol, 0.04% (w/v) bromophenol blue) was added to each 30 μl sample. Electrophoresis was carried out at room temperature (22° C) at constant voltage (8 V/cm) for 3 to 3.5 h. The gels were then stained for 15 min with ethidium bromide (2 μg/ml solution) and destained for 2−3 hrs at 4° C in buffer T + 2 M NaCl.

RESULTS

Stability of the scRPA hetero-trimer

To facilitate interpretation of our scRPA-ssDNA binding studies, we first examined the assembly state of the protein under the solution conditions used to examine DNA binding. Both sedimentation equilibrium and sedimentation velocity experiments were performed as described in Materials and Methods at five NaCl concentrations (20 mM, 0.2 M, 1.0 M, 1.5 M and 2.5 M NaCl) in buffer T at 25° C. The results of sedimentation equilibrium experiments performed in 20 mM and 1.5 M NaCl are shown in Figure 2A and 2B, respectively. All sedimentation equilibrium data were analyzed globally using non-linear least squares (NLLS) methods and all sedimentation profiles obtained at [NaCl] ≤ 1.5 M were well described by a model for a single ideal species (eq 1 with n = 1; see Materials and Methods) with average molecular masses close to that expected for an scRPA hetero-trimer (M_r = 114,000 Da) (see Table 1). In sedimentation velocity experiments performed in buffer T plus 20 mM NaCl at 25° C (data not shown) ([scRPA] = 1.2 μM), scRPA sediments as a single species with a weight average sedimentation coefficient, $\bar{S}_{20,w}$ = (5.64 ± 0.01) S, corresponding to a molecular mass of 105 ± 1 kDa as estimated by the program DCDT$^+$ (version 1.16, John S. Philo). However, at 2.5 M NaCl (buffer T, 25°C), ([scRPA] = 1.5 μM) a lower sedimentation coefficient of (5.05 ± 0.04) S was obtained, corresponding to a lower molecular mass of 62 ± 1 kDa. These results indicate that scRPA is a stable hetero-trimer at all [NaCl] less than or equal to 1.5 M, but that partial dissociation of the scRPA hetero-trimer appears to occur at 2.5 M NaCl.

We also examined the effects of 5 mM $MgCl_2$ and 1 mM DTT on the scRPA assembly state using sedimentation velocity (data not shown). In the presence of 20 mM NaCl (buffer T, 25° C), scRPA sedimented as a single species with weight average sedimentation coefficients of $\bar{S}_{20,w}$ = 5.63 ± 0.01 S and 5.61 ±0.02 S in the presence of 5mM $MgCl_2$ or 1mM DTT, respectively, corresponding to molecular masses of 105 ± 1 kDa, and 101 ± 2 (kDa), close to the expected value of 114 kDa.

Occluded site size of scRPA on poly(dT)

Any characterization of the ssDNA binding properties of a non-specific ssDNA binding protein such as scRPA should include a determination of the occluded site size (n) when bound to ssDNA. This is defined as the number of ssDNA nucleotides that are occluded by one protein and thus prevented from interacting with a second protein (62). As mentioned above, although such estimates have been reported for scRPA, these estimates vary considerably, from 20−95 nucleotides (29,48,49). Such variation might result from differences due to the technique or approach used for the measurement, or it could reflect real differences that result from effects of solution conditions. In fact, there is precedence for significant changes in the occluded site size for the *E. coli* SSB protein, a homo-tetrameric ssDNA binding protein, which can bind to ss-DNA in multiple binding modes that differ in occluded site size, from ~33 ± 2 to 65 ± 3 nucleotides (3,39,52,63). These different binding modes are influenced by the salt concentration and type, including cation valence, pH, temperature and protein binding density and reflect the fact that the *E. coli* SSB tetramer can bind to ss-DNA using either all four or only two of its subunits, each of which contains an OB-fold, while still remaining tetrameric. In fact, it has been hypothesized that RPA might also bind to ssDNA in multiple binding modes using different numbers of its OB-folds (37).

We therefore examined systematically the occluded site size for scRPA binding to the homopolynucleotide, poly(dT), as a function of salt concentration in order to determine if a similar binding mode transition exists for scRPA. We first examined the effect of NaCl concentration (0.02 − 1.5 M) on the apparent occluded site size for scRPA binding to poly(dT). The scRPA protein has 9 tryptophans (7 in RPA70, 1 in RPA32, and 1 in RPA14) (64), and the intrinsic tryptophan fluorescence of scRPA is partially quenched upon binding ssDNA (29,48). We therefore used this tryptophan fluorescence quenching to monitor scRPA binding to poly(dT). Poly(dT) was used for several reasons. First, it remains single stranded and does not form intramolecular base pairs under a wide range of solution conditions. Second, scRPA binds with high affinity to poly(dT) (48), thus facilitating measurements of the occluded site size (39). The occluded site size measurements were performed by titrating scRPA with poly (dT) and monitoring the scRPA Trp fluorescence intensity (see Materials and Methods).

The results of two titrations performed at different NaCl concentrations (20 mM and 1.5 M) are shown in Figure 3. In each case, the Trp fluorescence quenching increases as a linear function of the poly(dT) concentration, eventually reaching a plateau of ~40−44% quenching at high poly(dT) concentrations. The occluded site size (n) is estimated from these plots as the ratio of the moles of poly(dT) nucleotides per mole of scRPA at the intersection of the straight lines defining the increase in Trp fluorescence quenching and the plateau. Titrations at each [NaCl] were performed at two or more scRPA concentrations (from 40 to 300 nM) and the apparent stoichiometries were found to be independent of scRPA concentration indicating that binding is stoichiometric at each NaCl concentration.

Similar titrations were repeated at a series of [NaCl] from 20 mM to 1.5 M and the site sizes are plotted in Figure 3C. These data clearly show that the occluded site size (n_{app}) is affected by [NaCl]. A plateau value of n_{app} =18−20 nucleotides is observed for [NaCl] ≤ 100 mM, but above 100 mM NaCl, n_{app} increases with increasing [NaCl], reaching a value of ~26−28

nucleotides at 1.0 and 1.5 M NaCl (see also Table 2). The maximum extent of Trp fluorescence quenching is relatively constant for the titrations performed at each [NaCl], although some variation in the final extent of fluorescence quenching (43 − 50%) is observed for measurements at 20 mM NaCl. This variation suggests that there may be some slow kinetic processes occurring, possibly reflecting slow protein-DNA rearrangements at 20 mM NaCl. Titrations at 2.0 M NaCl were also performed, but the binding affinity was not sufficiently high to allow an unambiguous determination of the site size. Based on the fact that scRPA undergoes partial disassembly at 2.5 M NaCl (see above), it seems likely that this may also occur at 2.0 M NaCl. In any event, these data show clear evidence for a [NaCl]-dependent change in occluded site size for scRPA binding to poly(dT). The midpoint of the transition occurs at approximately 0.36 M NaCl.

scRPA binding to $(dT)_{30}$ (L ≥ n) examined by Isothermal Titration Calorimetry

If the change in occluded site size with increasing [NaCl] shown in Figure 3C reflects a change in the number of OB-folds that interact with the poly(dT), then this might also be detected as a change in the stoichiometry of scRPA binding to a ss-oligodeoxythymidylate of length near the occluded site size. To test this, we examined the binding of scRPA to the oligodeoxythymidylate, $(dT)_{30,}$ at high and low [NaCl]. Since the occluded site size is 18−20 nucleotides at low [NaCl] (0.02 to 0.2M), but increases to 26−28 nucleotides at high [NaCl] (above 1.0 M), then $(dT)_{30}$ might bind only one scRPA at high [NaCl], but two scRPA molecules at the lower [NaCl]. We examined this question using isothermal titration calorimetry (ITC), fluorescence titrations and sedimentation equilibrium.

We first performed ITC titrations of scRPA with $(dT)_{30}$ at three [NaCl] (0.02, 0.2 and 1.5 M) (buffer T, pH 8.1, 25° C) and the results are shown in Figure 4. The isotherm for scRPA binding to $(dT)_{30}$ obtained in 1.5 M NaCl (Figure 4A) is well described by a 1:1 binding model yielding an equilibrium binding constant, $K_{obs}= (1.2\pm0.1)\times10^8\ M^{-1}$ and a binding enthalpy, $\Delta H_{obs}= -46.2\pm0.5$ kcal/mol. However, at the lower salt concentration (20 mM NaCl) (Figure 4B), the shape of the binding isotherm is distinctly different. In addition, the binding enthalpy at excess scRPA (low values of $[(dT)_{30}]/[scRPA]$) is considerably more negative (~ −75 kcal/mole $(dT)_{30}$) in 20 mM NaCl than in 1.5 M NaCl (~ −46 kcal/mole). The data in Figure 4B indicate that two scRPA hetero-trimers are able to bind to a single $(dT)_{30}$ molecule. At low ratios of $[(dT)_{30}]_{tot}/[scRPA]_{tot}$ a mixture of 1:1 and 2:1 complexes exist; however, only 1:1 complex is observed at higher $[(dT)_{30}]_{tot}$. We note that the shape of the binding isotherm in Figure 4B indicates that the second scRPA molecule binds with lower apparent affinity than does the first one (apparent negative cooperativity), since saturation at $[(dT)_{30}]_{tot}/[scRPA]_{tot} = 0.5$ would be expected if binding of two scRPA molecules occurred with a large positive cooperativity. The titrations in Figure 4B can be fit to model in which two scRPA molecules bind sequentially to $(dT)_{30}$ (see Materials and methods) yielding $K_{1,obs} = (1.6\pm0.8)\times10^{10}M^{-1}$, $\Delta H_1=-56.5\pm0.5$ kcal/mol and $K_{2,obs} =(2.4\pm1.5)\times10^6\ _M{}^{-1}$, $\Delta H_2=-32\pm10$ kcal/mol.

The ability of $(dT)_{30}$ to bind two scRPA molecules is also apparent from titrations performed in 0.20 M NaCl (buffer T, pH 8.1, 10%(v/v) glycerol), where the estimated occluded site size on poly(dT) is low (n_{app} =21−22 nucleotides, see Table 2). In this case, we performed titrations in both the "forward" (titrating scRPA in the cell with $(dT)_{30}$ (Figure 4C)) and "reverse" (titrating $(dT)_{30}$ in the cell with scRPA (Figure 4D) directions. The isotherm in Figure 4C indicates that a second molecule of RPA binds to $(dT)_{30}$ at $[RPA]_{tot}/[(dT)_{30}]_{tot}>1$, although with lower macroscopic affinity, as judged by the gradual increase at $[RPA]_{tot}/[(dT)_{30}]_{tot}>>1$. The data in Figure 4C can be fit to a model for the sequential binding of two scRPA molecules (see Materials and Methods), yielding $K_{1,obs} = (9.3\pm5.6)\times10^8M^{-1}$, $\Delta H_1=-55.4\pm1.1$ kcal/mol and $K_{2,obs} = (6.0\pm5.2)\times10^5\ M^{-1}$, $\Delta H_2=-37\pm19$ kcal/mol. The isotherm obtained from the "reverse" titration shown in Figure 4D can also be fit to the same model yielding similar

parameters: $K_{1,obs} = (8.9\pm4.5)\times10^8\ M^{-1}$, $\Delta H_1 = -51.6\pm1.2$ kcal/mol and $K_{2,obs} = (5.3\pm5.5)\times10^5\ M^{-1}$, $\Delta H_2 = -30\pm22$ kcal/mol. The large uncertainties in the estimates for $K_{2,obs}$ and ΔH_2 are due to the low affinity and high correlation between these parameters. On the other hand, the estimate of ΔH_1 (−52 to −55 kcal/ mol) is more reliable due to the higher apparent affinity for the binding of the first scRPA molecule. These results indicate that the binding of the second scRPA molecule to $(dT)_{30}$ occurs with an apparent binding constant that is ~10^3-fold lower than for the binding of the first molecule of scRPA. However, much of this apparent lower affinity is likely due to the non-specific nature of the binding interaction, there are many more sites available on the DNA for binding of the first scRPA molecule ($30 - n + 1 = 13$, for the $n = 18$ mode of binding), than the single site available for the second scRPA molecule.

In general, these results are consistent with the effects of [NaCl] on the apparent site size for scRPA binding to poly(dT). Only one scRPA can bind to $(dT)_{30}$ at 1.5 M NaCl, where the occluded site size on poly(dT) is 26−28 nucleotides. However, at the lower [NaCl] (20 mM and 200 mM), where the occluded site size is only 18−20 nucleotides, two molecules of scRPA can bind to $(dT)_{30}$. These differences in site sizes and binding stoichiometries likely reflect the manifestation of alternative binding modes differing in the number of OB-folds that interact with the ssDNA.

Sedimentation Equilibrium Studies of scRPA binding to $(dT)_{30}$

To further examine the stoichiometries of scRPA-$(dT)_{30}$ complexes we performed sedimentation equilibrium experiments. For these studies we used $(dT)_{29}$ labeled covalently with Cy3 at its 5′ end (Cy3-$(dT)_{29}$). Since the Cy3 moiety has an absorbance peak at 550 nm, this enabled us to monitor the sedimentation profile of Cy3-$(dT)_{29}$ without interference from the scRPA. Complex formation between Cy3-$(dT)_{29}$ and scRPA is detectable as an increase in the weight average molecular mass (M_{app}) of the Cy3-$(dT)_{29}$, hence such experiments should readily differentiate ssDNA bound with one or two scRPA molecules. These studies were performed in buffer T (pH 8.1, 25° C) in the presence of either 20 mM NaCl or 1.5 M NaCl and at two molar ratios of $[scRPA]_{tot}$ to $[Cy3\text{-}(dT)_{29}]_{tot}$, one at a four-fold excess scRPA and another at a 1:1 molar ratio.

The sedimentation equilibrium profiles at 20 mM NaCl are shown in Figure 5A and 5B for the experiments performed at 1:1 and 4:1 molar ratios of scRPA to ssDNA, respectively. Both sets of data are described well by a single species model, as judged from the random distribution of residuals. The best non-linear least squares fit to the data at a 1:1 molar ratio yields a weight average molecular mass of 113.6 ± 1.0 kDa, whereas the best fit to the data at a 4:1 molar ratio yields a weight average molecular mass of 222.8 ± 2.0 kDa. The masses expected for Cy3-$(dT)_{29}$ bound with one or two scRPA molecules are 123 kDa and 218 kDa, respectevily. Hence, these results are consistent with the ITC experiments performed at the same NaCl concentration (20 mM), and indicate that a 1:1 complex can form at low [scRPA], but that a 2:1 complex can form at higher scRPA concentrations. On the other hand, sedimentation equilibrium experiments performed at 1.5 M NaCl indicate that only one scRPA can bind to the Cy3-$(dT)_{29}$ even at a 4:1 molar ratio (scRPA/5′-Cy3-$(dT)_{29}$) (see Figure 5C). The data in Figure 5C are well described by a single sedimenting species with a weight average molecular mass of 127.3 ± 2.9 kDa, consistent with a single scRPA bound per Cy3-$(dT)_{29}$.

We also determined the ability of scRPA to bind to $(dT)_{22}$ and $(dT)_{30}$ at low salt concentration (20mM NaCl) in buffer T by using an electrophoretic mobility shift assay (EMSA) (data not shown). The experiments indicate that only 1:1 complexes are formed when both oligodeoxynucleotides are present in excess over scRPA, whereas under conditions of excess protein, only one complex is formed with $(dT)_{22}$, whereas two bands are observed for scRPA binding to $(dT)_{30}$ at increasing ratios of $[scRPA]_{tot}/[ssDNA]_{tot}$ indicating that both 1:1 and 2:1 complexes can form with $(dT)_{30}$ under low [NaCl] conditions.

Stoichiometry of scRPA binding to short ss-oligodeoxynucleotides (L ≤ n) at 1.5 M NaCl examined by fluorescence quenching

The occluded site sizes, n=18−20 and n=26−28, determined for scRPA binding to poly(dT) at low and high salt concentrations, respectively suggest that a single scRPA protein could potentially bind more then one ss-oligodeoxynucleotide if the length of oligodeoxynucleotide, L, is less than n. To examine this we investigated a series of $(dT)_L$ with L varying from 16 to 28 nucleotides (i.e., with $L \leq n$). For these experiments we monitored $(dT)_L$ binding by the quenching of the scRPA Trp fluorescence. These experiments were performed at 1.5 M NaCl (buffer T, pH 8.1, 25°C). Experiments were also performed at 20 mM NaCl; however, those titrations displayed large variations in fluorescence quenching amplitudes and thus were not suitable for quantitative analysis. The experiments performed at 1.5 M NaCl were well behaved.

The binding of scRPA to $(dT)_L$, (for L = 28, 26, 22, 20, 18, and 16 nucleotides) was examined in 1.5 M NaCl (buffer T, pH 8.1, 25° C). Recall that the occluded site size, n, determined with poly(dT) is 26−28 nucleotides under these conditions (see Table 2). The results of scRPA titrations with $(dT)_{28}$ and $(dT)_{20}$ are shown in Figure 6A and 6C, respectively. In both cases two or more titrations were performed at different scRPA concentrations and the titrations were analyzed using the model independent binding density function analysis (59) to determine the relationship between the average fluorescence quenching signal and the average extent of $(dT)_L$ binding per scRPA. The results, plotted in Figure 6B (for $(dT)_{28}$) and Figure 6D (for $(dT)_{20}$), demonstrate that the average quenching increases linearly with the average extent of binding. Furthermore, a linear extrapolation of this line to the maximum fluorescence quenching observed at saturation (Q_{max}) (plateau values in Figure 6A and 6C) indicates a 1:1 stoichiometry of binding. The isotherms are well described by a one site binding model (see Materials and Methods), as are all of the isotherms for $(dT)_L$ with L = 20 − 28 nucleotides. Non-linear least squares analysis of these binding isotherms yields the observed equilibrium binding constant (K_{obs}) and Q_{max}, which are listed in Table 3 for $(dT)_L$, with L=20, 22, 26 and 28 nucleotides. K_{obs} decreases slightly (from $(6.7\pm0.4)\times10^7$ M^{-1} to $(4.0\pm0.4)\times10^7$ M^{-1}), as does Q_{max}, (from 0.38±0.01 to 0.30±0.01), as L decreases from 28 to 20 nucleotides. This behavior is expected since the shorter oligodeoxythymidylates interact with fewer residues within the protein binding site.

We next examined the binding of scRPA to $(dT)_L$ with L = 16 and 18 nucleotides. For these shorter oligodeoxynucleotides, we detect binding of a second ssDNA molecule to scRPA. Titrations of scRPA with $(dT)_{18}$ at two scRPA concentrations (0.10 μM and 0.36 μM) in 1.5 M NaCl (buffer T, pH 8.1, 25°C) are shown in Figure 7A. These titrations show clear biphasic behavior indicating that more than one $(dT)_{18}$ molecule can bind to scRPA. Analysis of these titrations using the model independent binding density function analysis (59) confirms a 2:1 binding stoichiometry (see Figure 7B). Binding of the first $(dT)_{18}$ results in a fluorescence quenching of $Q_1 \approx 0.20$, while binding of two $(dT)_{18}$ molecules results in a total quenching of $Q_2 \approx 0.33$. The data in Figure 7A can be globally fit to a two site binding model (see Materials and Methods) yielding macroscopic binding constants for the first $(dT)_{18}$ molecule, $K_{1,obs}$ = $(2.1\pm0.2)\times10^7$ M^{-1} and for the second $(dT)_{18}$ molecule, $K_{2,obs}$ = $(1.3\pm0.5)\times10^5$ M^{-1}, with corresponding values of quenching, Q_1=0.23±0.01 and Q_2=0.33±0.01 (see Table 3). Similar experiments performed with $(dT)_{16}$ also show that two moles of $(dT)_{16}$ can bind per mole of scRPA at saturation (data not shown).

The maximum stoichiometries for the binding of $(dT)_L$ as a function of L are plotted in Figure 7C. Clearly, for the binding of $(dT)_{16}$ or $(dT)_{18}$, there is sufficient room remaining within the scRPA binding site to form a stable interaction with at least part of a second oligodeoxynucleotide. In the case of $(dT)_{16}$ there may be as many as 12 nucleotides of the

second $(dT)_{16}$ molecule that can interact with scRPA. However, for $L \geq 20$ nucleotides, only 1:1 complexes are observed.

Estimation of the scRPA contact size by Isothermal Titration Calorimetry

The occluded site size, *n*, provides a measure of the number of nucleotides that are occluded by one scRPA upon binding to poly(dT), such that a second scRPA molecule is unable to access these nucleotides. The contact size, *m*, is defined as the number of contiguous nucleotides required to form all interactions with the protein, hence, $m \leq n$. In order to estimate the contact size for scRPA binding to ssDNA, we performed ITC titrations of scRPA with a series of $(dT)_L$ at 1.5 M NaCl (buffer T, pH 8.1) to determine how the equilibrium binding constant, K_{obs}, and the binding enthalpy, ΔH_{obs}, are affected by oligodeoxynucleotide length, *L*. The magnitude of ΔH_{obs} is expected to increase as the number of nucleotides involved in interactions with the protein increases until the contact site size, *m*, is reached.

Figure 8A shows representative data from an ITC experiment in which $(dT)_{28}$ was titrated into a solution of scRPA (0.24 μM) in 1.5 M NaCl (buffer T, 25 C). These data are replotted as the injection heats normalized to the amount of injected DNA in Figure 8B. The smooth curve in Figure 8B represents the best fit of these data to a 1:1 binding isotherm (eq 9) with equilibrium constant, $K_{obs} = (4.8 \pm 0.5) \times 10^7\ M^{-1}$ and $\Delta H_{obs} = -47.1 \pm 0.9$ kcal/mol. A series of such experiments were performed as a function of oligodeoxynucleotide length, for $L = 16$ to 34 nucleotides, and the ΔH_{obs} for binding of a single $(dT)_L$ are plotted as a function of *L* in Figure 8C. These results show that ΔH_{obs} decreases (becoming more negative) with a fairly linear dependence on *L* up to $L = 28$ nucleotides, and then levels off at $\Delta H_{obs} = -46 \pm 1$ kcal/mol. The contact site size (m) estimated from these data is ~28 nucleotides, which is equal to the occluded site size measured with poly(dT) under these same conditions.

Analysis of the ITC binding isotherms also yields the macroscopic equilibrium binding constants, $K_{obs,L}$, which are plotted as a function of *L* in Figure 8D. Two phases are observed in this plot. The values of $K_{obs,L}$ increase only slightly (by a factor of ~ 4) as *L* increases from 16 to 28 nucleotides, then increase more substantially as *L* increases from 28 to 34 nucleotides. The phase in the range, $L < m$, results from the fact that as *L* decreases, fewer contacts are made with the protein. The dependence of $K_{obs,L}$ on *L* in this region will depend on the nature of the ssDNA binding site within scRPA. The dependence of $K_{obs,L}$ on *L* in the range $L > m$ can be explained by the fact that scRPA is a non-specific DNA binding protein and thus the number of available binding sites for scRPA on $(dT)_L$ will increase as *L* increases and is expected to follow eq 9 (62, 65),

$$K_{obs,L} = K_{int}(L - m + 1) \tag{9}$$

where the intrinsic binding constant K_{int} is the binding constant for scRPA binding to an oligodeoxynucleotide with $L = m$. If we use eq 9 to describe the linear dependence of $K_{obs,L}$ on *L* from $L = 28$ to 34 nucleotides in Figure 8D, we estimate $m = \sim 27$ nucleotides, which is consistent with the estimate obtained from analysis of the data in Figure 8C. Both estimates of the contact size, *m*, are the same within our uncertainties as the estimate of the occluded site size, *n*, for scRPA binding at 1.5 M NaCl.

Effects of Salt Concentration on scRPA-$(dT)_{26}$ binding affinity

To obtain information about the electrostatic aspects of scRPA binding to ssDNA, we examined the effects of the monovalent salts, NaCl and NaBr, on the equilibrium constant, K_{obs}, for scRPA binding to $(dT)_{26}$. We chose to examine $(dT)_{26}$ since the occluded site size of scRPA is ~ 26−28 nucleotides at high [NaCl] (1.5 M). Binding was monitored by the quenching of the scRPA tryptophan fluorescence upon titration with $(dT)_{26}$ (buffer T, pH 8.1, 0.1mM EDTA, 25.0° C). The results of titrations performed as a function of [NaCl] and [NaBr] are shown in

Figure 9A and 9B, respectively. At each salt concentration, the binding isotherms are well described by a simple 1:1 binding model. For each salt type, as the salt concentration is increased the binding isotherms are shifted toward higher $(dT)_{26}$ concentrations, indicating that the binding constant decreases with increasing salt concentrations. In addition, the maximum fluorescence quenching accompanying saturation of scRPA with $(dT)_{26}$ decreases with increasing in salt concentration. The dependences of K_{obs} on [NaCl] and [NaBr] (log-log plots) are shown in Figure 9C. Both plots are linear over the salt concentration ranges examined, with slopes of $\partial \log K/\partial \log[NaCl] = -3.42 \pm 0.07$, and $\partial \log K/\partial[NaBr] = -3.87 \pm 0.15$, indicating that the binding of $(dT)_{26}$ is accompanied by a net release of 3−4 ions (cations and/or anions). Clearly, there is an effect of anion type in that the binding affinity is higher in the presence of Cl- than in the presence of Br-. Such effects have also been observed for the *E. coli* SSB protein binding to ssDNA (60, 66 , 67).

Cooperativity of scRPA binding to M13ssDNA is low

Single stranded binding proteins are commonly thought to bind cooperatively to long ssDNA and thus be capable of forming clusters of protein on ssDNA. This view stems primarily from the fact that the first SSB protein that was identified, the phage T4 gene 32 protein, shows highly cooperative binding to ssDNA (1,53). In addition, the *E. coli* SSB tetramer shows highly cooperative binding in its $(SSB)_{35}$ binding mode, although binding is not very cooperative in its fully wrapped $(SSB)_{65}$ binding mode (41,61,66). Studies examining the cooperativity of scRPA binding to ssDNA have been reported, although the conclusions have differed significantly. It was shown that both scRPA and hRPA bind to ssDNA with low cooperativity (nearest neighbor cooperativity parameter, $\omega = 10 - 20$) (48,68) using both fluorescence quenching and electrophoretic mobility shift assays (EMSA). However, using fluorescence quenching, Alani et al. (29) reported that binding of scRPA is highly cooperative, with $\omega = 10^4$ to 10^5. Since the different *E. coli* SSB binding modes display very different cooperativities for ssDNA binding, we wished to determine whether the two scRPA binding modes that we observe might also display different cooperativities.

The binding affinity of scRPA for poly(dT) is too high (stoichiometric binding) under all of the solution conditions examined here and thus we cannot obtain a quantitative estimate of the co-operativity for scRPA binding to poly(dT) under these conditions. To examine this issue qualitatively, we used an agarose gel electrophoresis assay described previously for examination of the cooperativity of *E. coli* SSB binding to single stranded DNA in its different binding modes (61). We examined the binding cooperativity of scRPA to circular M13mp18 ssDNA from bacteriophage M13 at two different [NaCl] (20 mM and 1.5 M) (see Materials and Methods). Complexes of scRPA with ssM13mp18 DNA were formed at varying scRPA to DNA ratios by directly mixing the scRPA and DNA in defined solution conditions (buffer T, 22°C) at a given [NaCl] and allowed to equilibrate for one hour before electrophoresis. The gels were run in a low salt buffer (pH 7.8, 20 mM-Tris, 0.4 mM sodium acetate, 0.2 mM Na_3EDTA) to minimize redistribution of scRPA molecules during electrophoresis. The scRPA-ssM13 DNA complexes were then electrophoresed in a 0.5% agarose gel, which separates the DNA molecules according to the amount of scRPA bound to each DNA molecule; the free ssDNA migrates fastest, and DNA with increasing amount of bound SSB migrates progressively slowest.

In this type of experiment, a protein that binds with very high cooperativity to DNA would yield a bimodal distribution of DNA molecules, consisting of two sharp bands representing DNA that was fully saturated with the protein and totally free DNA in the limit of large excess of nucleic acid (low binding density). A non-cooperatively binding protein, on the other hand, is expected to be distributed randomly among the ssDNA molecules and hence a single, more diffuse band should be observed at all binding densities. For the experiment performed at 20

mM NaCl, where the occluded site size is 18−20 nucleotides, the gel patterns show a broad binding density distribution and a single, somewhat diffuse band at each scRPA concentration indicating low cooperativity (see Figure 1S A in Supporting Information). The identical experiments performed at 1.5 M NaCl, where the occluded site size is ~28 nucleotides, also show a single, diffuse band at low ratios of scRPA to DNA (see Figure 1S B in Supporting Information). We note that the fluorescence titration experiments of Alani et al. (1992) (29) that were used to conclude that scRPA binds with high cooperativity to ssDNA were performed in the presence of high $MgCl_2$ concentrations (140 − 160 mM). We therefore also examined scRPA binding to ssDNA under these conditions using the agarose gel electrophoresis assay, but observed similar low cooperativity behavior as in the absence of $MgCl_2$. Therefore, we find that scRPA binding to ssDNA under these conditions does not exhibit highly cooperativity binding to ssDNA, which is consistent with reports that cooperativity of scRPA binding to ssDNA is only low or moderate (48).

DISCUSSION

The eukaryotic RPA protein plays a central role in DNA metabolism (5). The hetero-trimeric protein contains six OB-folds (see Figure 1) and thus six potential ssDNA binding domains. Based on this, there has been speculation concerning whether all or only a subset of these OB-folds interact with ssDNA and whether RPA might use different subsets of these OB-folds to bind ssDNA in alternate “binding modes”. In fact, such multiple binding modes have been observed for the homo-tetrameric *E. coli* SSB protein, which contains four OB-folds (one per subunit). At least two of the *E. coli* SSB binding modes differ by the number of subunits that interact with the ssDNA (3,4). The binding properties of the different *E. coli* SSB binding modes differ substantially, including both site size and inter-tetramer cooperativity (3). Philipova et al. (37) first recognized that RPA contains at least four OB-folds and by analogy with the *E. coli* SSB protein suggested that RPA may also bind to ssDNA using multiple binding modes differing by the number of OB-folds used to contact the ssDNA.

Based on studies of oligodeoxynucleotide binding to human RPA (hsRPA), it was proposed that hsRPA can bind to ssDNA in two binding modes, an unstable 8 nt mode, observable only by crosslinking studies and a larger stable 30 nt binding mode (28,69). Measurements of the ssDNA binding site size for RPA have been reported for a number of other organisms, although the reported values vary considerably from 22 nt for *D. melanogaster* (32), 20−25 nt for calf (30), and the largest range of values has been reported for yeast, from 20−30 nt (49) to 45 nt (48) to 90 nt (29). By systematically mutating each OB-fold, Bastin-Shanower (2001) (27) concluded that OB-folds A, B and C interact with 12 nt and that OB-fold D also interacts with ssDNA, but only when it is longer than 23 nt. Recent reviews of RPA structure suggest that OB-folds A and B interact with 8−10 nt, A, B and C interact with 13−14 nt and all four OB-folds (A, B, C and D) occlude 30 nt. Others have concluded that two binding modes exist, the 8 nt unstable mode and the 30 nt stable mode (50). In addition to the confusion concerning the different reported site sizes and potential binding modes, no previous studies have provided evidence that RPA can bind to ssDNA in stable alternate binding modes or that RPA can undergo reversible transitions between alternate binding modes.

In the study reported here, we used four approaches and three techniques to examine the modes of scRPA binding to ssDNA. These experiments were performed with scRPA that was purified using a ssDNA cellulose column as the last purification step, hence all of the scRPA was selected for ssDNA binding activity and thus it was not necessary to correct for the presence of inactive scRPA. The approaches used included direct measurements of the occluded site size on poly(dT) by monitoring the number of nucleotides needed to saturate the scRPA tryptophan fluorescence quenching. We also examined the equilibrium binding of scRPA to a series of ss-oligodeoxythymidylates, $(dT)_L$, using sedimentation equilibrium, ITC and

fluorescence to measure both the equilibrium binding constant and ΔH_{obs} of binding as a function of length, *L*. Each of these sets of experiments indicates that scRPA can undergo a salt-dependent transition between two stable ssDNA binding modes *in vitro*.

One binding mode has an occluded site size of 18−20 nucleotides and is favored at low salt, while a second binding mode has a larger occluded site size of 26−28 nucleotides and is stabilized at [NaCl] > 500 mM. When combined with previous studies (27), it seems most likely that the low site size mode involves ssDNA interactions with OB-folds A, B and C only within RPA70, while the higher site size mode involves those as well as additional interactions with OB-fold D within RPA32, as depicted in Figure 10. This is also consistent with the available structural information that a single OB-fold binds ~ 4 nucleotides, while an additional two nucleotides are needed to bridge the gap between two OB-folds (21,70). This structural information predicts that 16−17 nucleotides would be needed to bind three OB-folds in tandem (e.g., A, B, C), consistent with the observed site size of 18−20 nucleotides at 20 mM NaCl. This simple analysis would then suggest that the number of nucleotides needed to bind contiguously to four OB folds (A, B, C, and D) is ~ 22−23 nucleotides. However, since the fourth OB-fold (D) is located in a different subunit (RPA32), the number of nucleotides needed to bridge the gap between the C and D OB-fold is expected to be more than ~ 2 nucleotides. Therefore, the larger site size of 26−28 nucleotides measured at 1.5 M NaCl is consistent with the involvement of OB-folds A, B, C and D. Most RPA binding studies suggest that OB-fold E (RPA14) does not interact with ssDNA (36), while OB-fold F appears to be primarily involved in protein-protein interactions (71,72). However, we cannot rule out that OB-fold F also interacts with ss-DNA in the higher site size binding mode.

We find no evidence for the putative 8 nucleotide binding mode, consistent with it not being a stable binding mode. In fact, the previous studies simply indicated that an 8 nucleotide long ssDNA could be crosslinked with glutaraldehyde to hsRPA (28). Such experiments cannot in general be used as a measure of a site size and also do not represent evidence for a distinct binding mode. Rather it simply indicates that a short oligodeoxynucleotide can be crosslinked to hsRPA.

The observation of a salt-dependent change in binding mode for scRPA has precedence in another SSB protein. The *E. coli* SSB homo-tetramer can bind to ssDNA in multiple binding modes differing in both occluded site size and cooperativity (3).However, the salt dependent increase in the occluded site size observed for scRPA, from 18−20 nucleotides to 26−28 nucleotides, is not as dramatic as for the *E. coli* SSB protein (33 to 65 nucleotides) (39). Whereas the scRPA binding mode transition appears to involve a switch from a mode using three OB-folds to bind ssDNA to a mode using four OB-folds, the *E. coli* SSB protein undergoes a transition from a mode using two OB-folds to one using four OB-folds. However, in both cases, the presence of multiple OB-folds within the protein is the feature that allows for these binding mode transitions.

The molecular basis for the binding mode switch in scRPA, as well as any potential functional role for the two modes is not known. In the case of *E. coli* SSB, two of the modes differ dramatically in their abilities to bind cooperatively to ssDNA (41,61). In addition, there is a salt-dependent negative cooperativity for ssDNA binding within the *E. coli* SSB tetramer (67,73,74). This results in a much lower affinity for ssDNA for binding to the second two subunits (OB-folds) within the tetramer. However, this negative cooperativity diminishes with increasing salt concentration, making it easier to bind ssDNA to all four subunits as the salt concentration increases, with a corresponding increase in site size when bound to long ssDNA. It remains to be seen whether a similar negative cooperativity exists within scRPA.

Previous studies of the cooperative binding of multiple RPA molecules to long ssDNA have also reported conflicting results. Most studies have concluded that RPA binds with little or moderate cooperativity (25,26,30,32). However, Alani et al. (29), reported a very high positive cooperativity ($\omega = 10^4 - 10^5$) for scRPA binding to ssDNA. In addition, Blackwell and Borowiec (28) concluded that hsRPA binds cooperatively in its 8 nt "binding mode". We examined this issue qualitatively by agarose gel electrophoresis of scRPA-ssM13 phage complexes, which allowed us to observe the distribution of protein on the DNA, which has been used to identify proteins that bind with very high cooperativity to DNA (61). We always observed protein distributions on the ssDNA that indicated the absence of high cooperativity at both low and high [NaCl] (20 mM and 1.5 M), as well as in the presence of high concentrations of $MgCl_2$. Thus, at equilibrium, the scRPA protein does not appear to bind with very high cooperativity under our solution conditions in either binding mode. Our ITC and sedimentation equilibrium studies also support this conclusion and thus agree with the studies of Sibenaller et al. (48).

The results presented here demonstrate that scRPA can bind to long ssDNA in at least two binding modes *in vitro* and that the relative stability of these two modes is influenced by salt concentration. Currently, there is no information available concerning which of these two modes, or whether possibly both, functions *in vivo*. However, in this context, it is also conceivable that other processes, such as post-translational modifications of RPA subunits, or interactions with accessory proteins, could influence the relative stability of the RPA binding modes, since such modifications are known to modulate the role of RPA in DNA metabolism. For example, phosphorylation of RPA is believed to switch off DNA replication, but stimulate DNA repair processes (75,76). In fact, the RPA32 subunit, containing OB-fold D and the major sites for phosphorylation, does possess ssDNA binding activity (27,77,78), and recent studies have emphasized the role of RPA32 in many important processes such as DNA repair (79) and DNA replication (77). Therefore, it is possible that the higher site size binding mode reported here, which appears to be due to the additional interaction with ssDNA of the RPA32 OB fold, may have a physiological role in DNA metabolism. It is also possible that phosphorylation of RPA32 may modulate both its DNA binding affinity and the relative stability of the different binding modes. Interestingly, recent studies show that a hyper-phosphorylated form of hsRPA, in which five sites on the 70 kDa and five sites on the 32 kDa subunits are phosphorylated, appears to have slightly reduced affinity for purine rich ssDNA (76).

Supplementary Material

Refer to Web version on PubMed Central for supplementary material.

ACKNOWLEDGMENT

We thank Dr. Marc Wold for his generous gift of the scRPA expression vector and for very useful discussions with him and Dr. Peter Burgers. We thank T. Ho for synthesis and purification of the oligodeoxynucleotides used in this study and Dr. Anita Niedziela-Majka for assistance with the analytical ultracentrifugation experiments. This research was supported in part by the NIH (RO1 GM30498).

Abbreviations

scRPA, Yeast Single Stranded DNA binding protein; ssDNA, single stranded DNA; OB fold, Oligosaccharide/Oligopeptide/Oligonucleotide Binding Fold; ITC, isothermal titration calorimetry; Tris, tris(hydroxymethyl)aminomethane; HEPES, 4-(hydroxyethyl)-1-piperazineethanesulfonic acid; EDTA, (ethylenediaminetetraacetic acid).

REFERENCES

1. Alberts B, Frey L, Delius H. Isolation and characterization of gene 5 protein of filamentous bacterial viruses. J Mol Biol 1972;68:139–152. [PubMed: 4115107]
2. Kowalczykowski, SC.; Bear, DG.; von Hippel, PH. Enzymes. 3rd Ed. XIV. 1981a. p. 373-444.
3. Lohman TM, Ferrari ME. Escherichia coli single-stranded DNA-binding protein: multiple DNA-binding modes and cooperativities. Annu Rev Biochem 1994;63:527–570. [PubMed: 7979247]
4. Raghunathan S, Kozlov AG, Lohman TM, Waksman G. Structure of the DNA binding domain of E. coli SSB bound to ssDNA. Nat Struct Biol 2000;7:648–652. [PubMed: 10932248]
5. Wold MS. Replication protein A: a heterotrimeric, single-stranded DNA-binding protein required for eukaryotic DNA metabolism. Annu Rev Biochem 1997;66:61–92. [PubMed: 9242902]
6. Iftode C, Daniely Y, Borowiec JA. Replication protein A (RPA): the eukaryotic SSB. Crit Rev Biochem Mol Biol 1999;34:141–180. [PubMed: 10473346]
7. Kenny MK, Lee SH, Hurwitz J. Multiple functions of human single-stranded-DNA binding protein in simian virus 40 DNA replication: single-strand stabilization and stimulation of DNA polymerases alpha and delta. Proc Natl Acad Sci U S A 1989;86:9757–9761. [PubMed: 2557626]
8. Brill SJ, Stillman B. Yeast replication factor-A functions in the unwinding of the SV40 origin of DNA replication. Nature 1989;342:92–95. [PubMed: 2554144]
9. Braun KA, Lao Y, He Z, Ingles CJ, Wold MS. Role of protein-protein interactions in the function of replication protein A (RPA): RPA modulates the activity of DNA polymerase alpha by multiple mechanisms. Biochemistry 1997;36:8443–8454. [PubMed: 9214288]
10. Wakasugi M, Shimizu M, Morioka H, Linn S, Nikaido O, Matsunaga T. Damaged DNA-binding protein DDB stimulates the excision of cyclobutane pyrimidine dimers in vitro in concert with XPA and replication protein A. J Biol Chem 2001;276:15434–15440. [PubMed: 11278856]
11. de Laat WL, Appeldoorn E, Sugasawa K, Weterings E, Jaspers NG, Hoeijmakers JH. DNA-binding polarity of human replication protein A positions nucleases in nucleotide excision repair. Genes Dev 1998;12:2598–2609. [PubMed: 9716411]
12. He Z, Henricksen LA, Wold MS, Ingles CJ. RPA involvement in the damage-recognition and incision steps of nucleotide excision repair. Nature 1995;374:566–569. [PubMed: 7700386]
13. Golub EI, Gupta RC, Haaf T, Wold MS, Radding CM. Interaction of human rad51 recombination protein with single-stranded DNA binding protein, RPA. Nucleic Acids Res 1998;26:5388–5393. [PubMed: 9826763]
14. Brosh RM Jr. Li JL, Kenny MK, Karow JK, Cooper MP, Kureekattil RP, Hickson ID, Bohr VA. Replication protein A physically interacts with the Bloom's syndrome protein and stimulates its helicase activity. J Biol Chem 2000;275:23500–23508. [PubMed: 10825162]
15. Brosh RM Jr. Orren DK, Nehlin JO, Ravn PH, Kenny MK, Machwe A, Bohr VA. Functional and physical interaction between WRN helicase and human replication protein A. J Biol Chem 1999;274:18341–18350. [PubMed: 10373438]
16. Li R, Botchan MR. The acidic transcriptional activation domains of VP16 and p53 bind the cellular replication protein A and stimulate in vitro BPV-1 DNA replication. Cell 1993;73:1207–1221. [PubMed: 8390328]
17. Cho JM, Song DJ, Bergeron J, Benlimame N, Wold MS, Alaoui-Jamali MA. RBT1, a novel transcriptional co-activator, binds the second subunit of replication protein A. Nucleic Acids Res 2000;28:3478–3485. [PubMed: 10982866]
18. Miller SD, Moses K, Jayaraman L, Prives C. Complex formation between p53 and replication protein A inhibits the sequence-specific DNA binding of p53 and is regulated by single-stranded DNA. Mol Cell Biol 1997;17:2194–2201. [PubMed: 9121469]
19. He Z, Brinton BT, Greenblatt J, Hassell JA, Ingles CJ. The transactivator proteins VP16 and GAL4 bind replication factor A. Cell 1993;73:1223–1232. [PubMed: 8513504]
20. Murzin AG. OB(oligonucleotide/oligosaccharide binding)-fold: common structural and functional solution for non-homologous sequences. Embo J 1993;12:861–867. [PubMed: 8458342]
21. Bochkarev A, Pfuetzner RA, Edwards AM, Frappier L. Structure of the single-stranded-DNA-binding domain of replication protein A bound to DNA. Nature 1997;385:176–181. [PubMed: 8990123]

22. Kerr ID, Wadsworth RI, Cubeddu L, Blankenfeldt W, Naismith JH, White MF. Insights into ssDNA recognition by the OB fold from a structural and thermodynamic study of Sulfolobus SSB protein. Embo J 2003;22:2561–2570. [PubMed: 12773373]
23. Brill SJ, Bastin-Shanower S. Identification and characterization of the fourth single-stranded-DNA binding domain of replication protein A. Mol Cell Biol 1998;18:7225–7234. [PubMed: 9819409]
24. Arunkumar AI, Stauffer ME, Bochkareva E, Bochkarev A, Chazin WJ. Independent and coordinated functions of replication protein A tandem high affinity single-stranded DNA binding domains. J Biol Chem 2003;278:41077–41082. [PubMed: 12881520]
25. Kim C, Paulus BF, Wold MS. Interactions of human replication protein A with oligonucleotides. Biochemistry 1994;33:14197–14206. [PubMed: 7947831]
26. Kim C, Snyder RO, Wold MS. Binding properties of replication protein A from human and yeast cells. Mol Cell Biol 1992;12:3050–3059. [PubMed: 1320195]
27. Bastin-Shanower SA, Brill SJ. Functional analysis of the four DNA binding domains of replication protein A. The role of RPA2 in ssDNA binding. J Biol Chem 2001;276:36446–36453. [PubMed: 11479296]
28. Blackwell LJ, Borowiec JA. Human replication protein A binds single-stranded DNA in two distinct complexes. Mol Cell Biol 1994;14:3993–4001. [PubMed: 8196638]
29. Alani E, Thresher R, Griffith JD, Kolodner RD. Characterization of DNA-binding and strand-exchange stimulation properties of y-RPA, a yeast single-strand-DNA-binding protein. J Mol Biol 1992;227:54–71. [PubMed: 1522601]
30. Atrazhev A, Zhang S, Grosse F. Single-stranded DNA binding protein from calf thymus. Purification, properties, and stimulation of the homologous DNA-polymerase-alpha-primase complex. Eur J Biochem 1992;210:855–865. [PubMed: 1483469]
31. Brown GW, Melendy TE, Ray DS. Conservation of structure and function of DNA replication protein A in the trypanosomatid Crithidia fasciculata. Proc Natl Acad Sci U S A 1992;89:10227–10231. [PubMed: 1332038]
32. Mitsis PG, Kowalczykowski SC, Lehman IR. A single-stranded DNA binding protein from Drosophila melanogaster: characterization of the heterotrimeric protein and its interaction with single-stranded DNA. Biochemistry 1993;32:5257–5266. [PubMed: 8494903]
33. Gomes XV, Wold MS. Functional domains of the 70-kilodalton subunit of human replication protein A. Biochemistry 1996;35:10558–10568. [PubMed: 8756712]
34. Walther AP, Gomes XV, Lao Y, Lee CG, Wold MS. Replication protein A interactions with DNA. 1. Functions of the DNA-binding and zinc-finger domains of the 70-kDa subunit. Biochemistry 1999;38:3963–3973. [PubMed: 10194308]
35. Bochkarev A, Bochkareva E, Frappier L, Edwards AM. The crystal structure of the complex of replication protein A subunits RPA32 and RPA14 reveals a mechanism for single-stranded DNA binding. Embo J 1999;18:4498–4504. [PubMed: 10449415]
36. Kolpashchikov DM, Weisshart K, Nasheuer HP, Khodyreva SN, Fanning E, Favre A, Lavrik OI. Interaction of the p70 subunit of RPA with a DNA template directs p32 to the 3′-end of nascent DNA. FEBS Lett 1999;450:131–134. [PubMed: 10350071]
37. Philipova D, Mullen JR, Maniar HS, Lu J, Gu C, Brill SJ. A hierarchy of SSB protomers in replication protein A. Genes Dev 1996;10:2222–2233. [PubMed: 8804316]
38. Griffith JD, Harris LD, Register J 3rd. Visualization of SSB-ssDNA complexes active in the assembly of stable RecA-DNA filaments. Cold Spring Harb Symp Quant Biol 1984;49:553–559. [PubMed: 6397310]
39. Lohman TM, Overman LB. Two binding modes in Escherichia coli single strand binding protein-single stranded DNA complexes. Modulation by NaCl concentration. J Biol Chem 1985;260:3594–3603. [PubMed: 3882711]
40. Lohman, TM.; Bujalowski, W. Escherichia coli single strand binding protein: Multiple single-stranded DNA binding modes and cooperativities. In: Revzin, A., editor. The Biology of Nonspecific DNA-Protein Interactions. CRC Press; Boca Raton, Fla: 1990. p. 131-170.
41. Ferrari ME, Bujalowski W, Lohman TM. Co-operative binding of Escherichia coli SSB tetramers to single-stranded DNA in the (SSB)35 binding mode. J Mol Biol 1994;236:106–123. [PubMed: 8107097]

42. Lohman TM, Bujalowski W. Effects of base composition on the negative cooperativity and binding mode transitions of Escherichia coli SSB-single-stranded DNA complexes. Biochemistry 1994;33:6167–6176. [PubMed: 8193130]
43. Bujalowski W, Overman LB, Lohman TM. Binding mode transitions of Escherichia coli single strand binding protein-single-stranded DNA complexes. Cation, anion, pH, and binding density effects. J Biol Chem 1988;263:4629–4640. [PubMed: 3280566]
44. Wei TF, Bujalowski W, Lohman TM. Cooperative binding of polyamines induces the Escherichia coli single-strand binding protein-DNA binding mode transitions. Biochemistry 1992;31:6166–6174. [PubMed: 1627560]
45. Overman LB, Lohman TM. Linkage of pH, anion and cation effects in protein-nucleic acid equilibria. Escherichia coli SSB protein-single stranded nucleic acid interactions. J Mol Biol 1994;236:165–178. [PubMed: 8107102]
46. Bochkareva E, Belegu V, Korolev S, Bochkarev A. Structure of the major single-stranded DNA-binding domain of replication protein A suggests a dynamic mechanism for DNA binding. Embo J 2001;20:612–618. [PubMed: 11157767]
47. Seroussi E, Lavi S. Replication protein A is the major single-stranded DNA binding protein detected in mammalian cell extracts by gel retardation assays and UV cross-linking of long and short single-stranded DNA molecules. J Biol Chem 1993;268:7147–7154. [PubMed: 8463251]
48. Sibenaller ZA, Sorensen BR, Wold MS. The 32- and 14-kilodalton subunits of replication protein A are responsible for species-specific interactions with single-stranded DNA. Biochemistry 1998;37:12496–12506. [PubMed: 9730822]
49. Sugiyama T, Zaitseva EM, Kowalczykowski SC. A single-stranded DNA-binding protein is needed for efficient presynaptic complex formation by the Saccharomyces cerevisiae Rad51 protein. J Biol Chem 1997;272:7940–7945. [PubMed: 9065463]
50. Krejci L, Sung P. RPA not that different from SSB. Structure 2002;10:601–602. [PubMed: 12015141]
51. Bochkarev A, Bochkareva E. From RPA to BRCA2: lessons from single-stranded DNA binding by the OB-fold. Curr Opin Struct Biol 2004;14:36–42. [PubMed: 15102447]
52. Bujalowski W, Lohman TM. Escherichia coli single-strand binding protein forms multiple, distinct complexes with single-stranded DNA. Biochemistry 1986;25:7799–7802. [PubMed: 3542037]
53. Kowalczykowski SC, Lonberg N, Newport JW, von Hippel PH. Interactions of bacteriophage T4-coded gene 32 protein with nucleic acids. I. Characterization of the binding interactions. J Mol Biol 1981;145:75–104. [PubMed: 7265204]
54. Berkowitz SA, Day LA. Molecular weight of single-stranded fd bacteriophage DNA. High speed equilibrium sedimentation and light scattering measurements. Biochemistry 1974;13:4825–4831. [PubMed: 4429667]
55. Kozlov AG, Lohman TM. Stopped-flow studies of the kinetics of single-stranded DNA binding and wrapping around the Escherichia coli SSB tetramer. Biochemistry 2002;41:6032–6044. [PubMed: 11993998]
56. Ralston, G. Introduction to Analytical Ultracentrifugation. I. Beckman Instruments, Inc; 1993.
57. Maluf NK, Lohman TM. Self-association equilibria of Escherichia coli UvrD helicase studied by analytical ultracentrifugation. J Mol Biol 2003;325:889–912. [PubMed: 12527298]
58. Lohman TM, Mascotti DP. Nonspecific ligand-DNA equilibrium binding parameters determined by fluorescence methods. Methods Enzymol 1992;212:424–458. [PubMed: 1518458]
59. Lohman TM, Bujalowski W. Thermodynamic methods for model-independent determination of equilibrium binding isotherms for protein-DNA interactions: spectroscopic approaches to monitor binding. Methods Enzymol 1991;208:258–290. [PubMed: 1779838]
60. Kozlov AG, Lohman TM. Calorimetric studies of E. coli SSB protein-single-stranded DNA interactions. Effects of monovalent salts on binding enthalpy. J Mol Biol 1998;278:999–1014. [PubMed: 9600857]
61. Lohman TM, Overman LB, Datta S. Salt-dependent changes in the DNA binding co-operativity of Escherichia coli single strand binding protein. J Mol Biol 1986;187:603–615. [PubMed: 3519979]
62. McGhee JD, von Hippel PH. Theoretical aspects of DNA-protein interactions: co-operative and non-co-operative binding of large ligands to a one-dimensional homogeneous lattice. J Mol Biol 1974;86:469–489. [PubMed: 4416620]

63. Chrysogelos S, Griffith J. Escherichia coli single-strand binding protein organizes single-stranded DNA in nucleosome-like units. Proc Natl Acad Sci U S A 1982;79:5803–5807. [PubMed: 6764531]
64. Brill SJ, Stillman B. Replication factor-A from Saccharomyces cerevisiae is encoded by three essential genes coordinately expressed at S phase. Genes Dev 1991;5:1589–1600. [PubMed: 1885001]
65. Epstein IR. Cooperative and non-cooperative binding of large ligands to a finite one-dimensional lattice. A model for ligand-oligonucleotide interactions. Biophys Chem 1978;8:327–339. [PubMed: 728537]
66. Overman LB, Bujalowski W, Lohman TM. Equilibrium binding of Escherichia coli single-strand binding protein to single-stranded nucleic acids in the (SSB)65 binding mode. Cation and anion effects and polynucleotide specificity. Biochemistry 1988;27:456–471. [PubMed: 3280021]
67. Bujalowski W, Lohman TM. Negative co-operativity in Escherichia coli single strand binding protein-oligonucleotide interactions. II. Salt, temperature and oligonucleotide length effects. J Mol Biol 1989;207:269–288. [PubMed: 2661833]
68. Kim C, Wold MS. Recombinant human replication protein A binds to polynucleotides with low cooperativity. Biochemistry 1995;34:2058–2064. [PubMed: 7849064]
69. Blackwell LJ, Borowiec JA, Masrangelo IA. Single-stranded-DNA binding alters human replication protein A structure and facilitates interaction with DNA-dependent protein kinase. Mol Cell Biol 1996;16:4798–4807. [PubMed: 8756638]
70. Bochkareva E, Korolev S, Lees-Miller SP, Bochkarev A. Structure of the RPA trimerization core and its role in the multistep DNA-binding mechanism of RPA. Embo J 2002;21:1855–1863. [PubMed: 11927569]
71. Yang H, Jeffrey PD, Miller J, Kinnucan E, Sun Y, Thoma NH, Zheng N, Chen PL, Lee WH, Pavletich NP. BRCA2 function in DNA binding and recombination from a BRCA2-DSS1-ssDNA structure. Science 2002;297:1837–1848. [PubMed: 12228710]
72. Stauffer ME, Chazin WJ. Structural mechanisms of DNA replication, repair, and recombination. J Biol Chem 2004;279:30915–30918. [PubMed: 15090549]
73. Lohman TM, Bujalowski W. Negative cooperativity within individual tetramers of Escherichia coli single strand binding protein is responsible for the transition between the (SSB)35 and (SSB)56 DNA binding modes. Biochemistry 1988;27:2260–2265. [PubMed: 3289611]
74. Bujalowski W, Lohman TM. Negative co-operativity in Escherichia coli single strand binding protein-oligonucleotide interactions. I. Evidence and a quantitative model. J Mol Biol 1989;207:249–268. [PubMed: 2661832]
75. Nuss JE, Patrick SM, Oakley GG, Alter GM, Robison JG, Dixon K, Turchi JJ. DNA damage induced hyperphosphorylation of replication protein A. 1. Identification of novel sites of phosphorylation in response to DNA damage. Biochemistry 2005;44:8428–8437. [PubMed: 15938632]
76. Patrick SM, Oakley GG, Dixon K, Turchi JJ. DNA damage induced hyperphosphorylation of replication protein A. 2. Characterization of DNA binding activity, protein interactions, and activity in DNA replication and repair. Biochemistry 2005;44:8438–8448. [PubMed: 15938633]
77. Mass G, Nethanel T, Kaufmann G. The middle subunit of replication protein A contacts growing RNA-DNA primers in replicating simian virus 40 chromosomes. Mol Cell Biol 1998;18:6399–6407. [PubMed: 9774655]
78. Lavrik OI, Nasheuer HP, Weisshart K, Wold MS, Prasad R, Beard WA, Wilson SH, Favre A. Subunits of human replication protein A are crosslinked by photoreactive primers synthesized by DNA polymerases. Nucleic Acids Res 1998;26:602–607. [PubMed: 9421522]
79. Elmayan T, Proux F, Vaucheret H. Arabidopsis RPA2: a genetic link among transcriptional gene silencing, DNA repair, and DNA replication. Curr Biol 2005;15:1919–1925. [PubMed: 16271868]

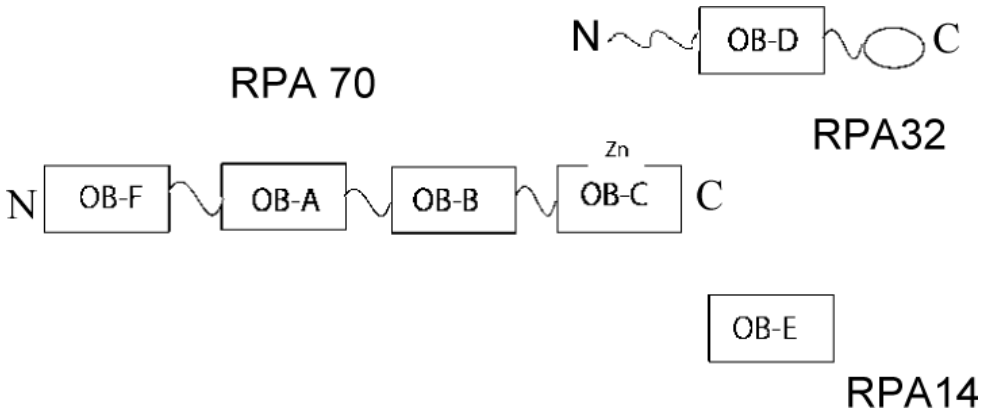

Figure 1.
Schematic representation of scRPA hetero-trimer with its six OB-folds. Four OB-folds are contained within RPA70 (OB-folds, A, B, C and F), one within RPA32 (OB-fold D), and one within RPA14 (OB-fold E).

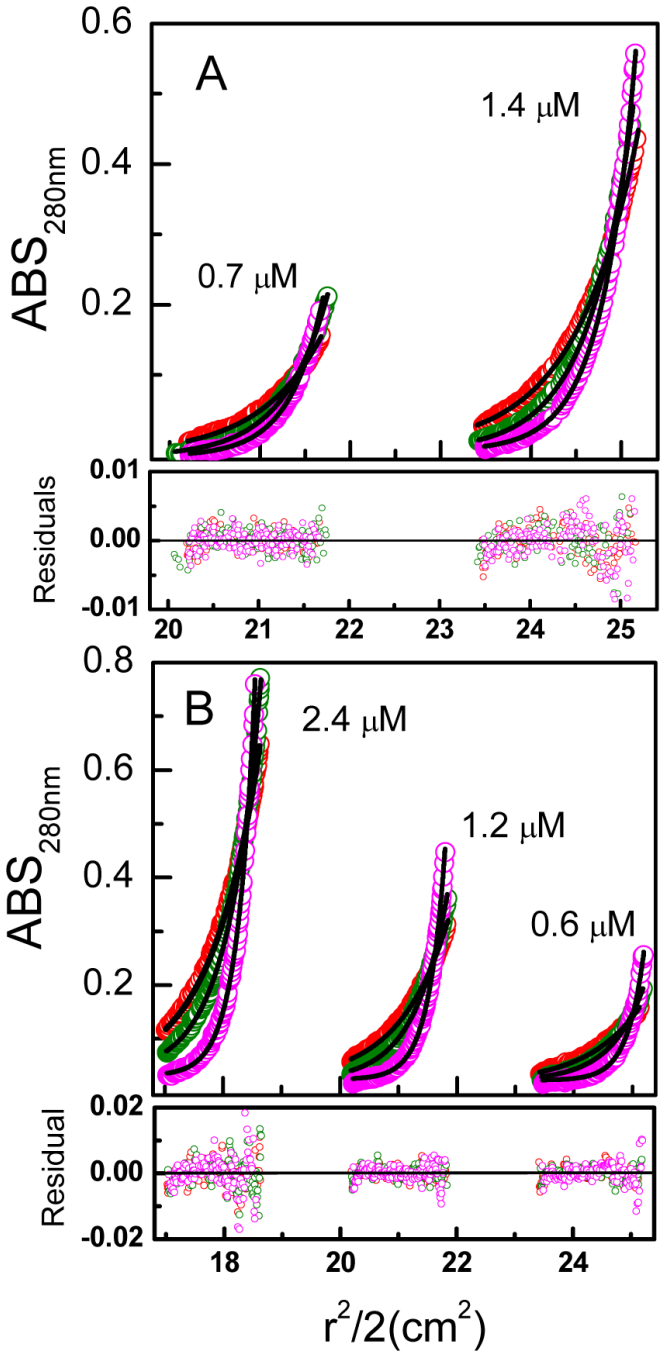

Figure 2. Stability of the scRPA heterotrimer as a function of [NaCl]

(A) - sedimentation equilibrium results at 20mM NaCl (buffer T, 25°C) for two scRPA concentrations (0.7 μM and 1.4 μM) and three rotor speeds of 10 krpm (red), 12 krpm (green), and 14 krpm (magenta). The solid curves represent the best global fits to a single species model with weight average molecular mass, M= 115 ± 4.7 kDa. (B) - sedimentation equilibrium results at 1.5 M NaCl (buffer T, 25°C) for three scRPA concentrations (2.4 μM, 1.2 μM, 0.6 μM) and three rotor speeds 10 krpm (red), 14 krpm (olive), 17 krpm (magenta). The solid curves represent the best global fits to a single species model with weight average molecular mass, M= 122 ± 3.8 kDa. The residuals for the fits are also shown below each data set.

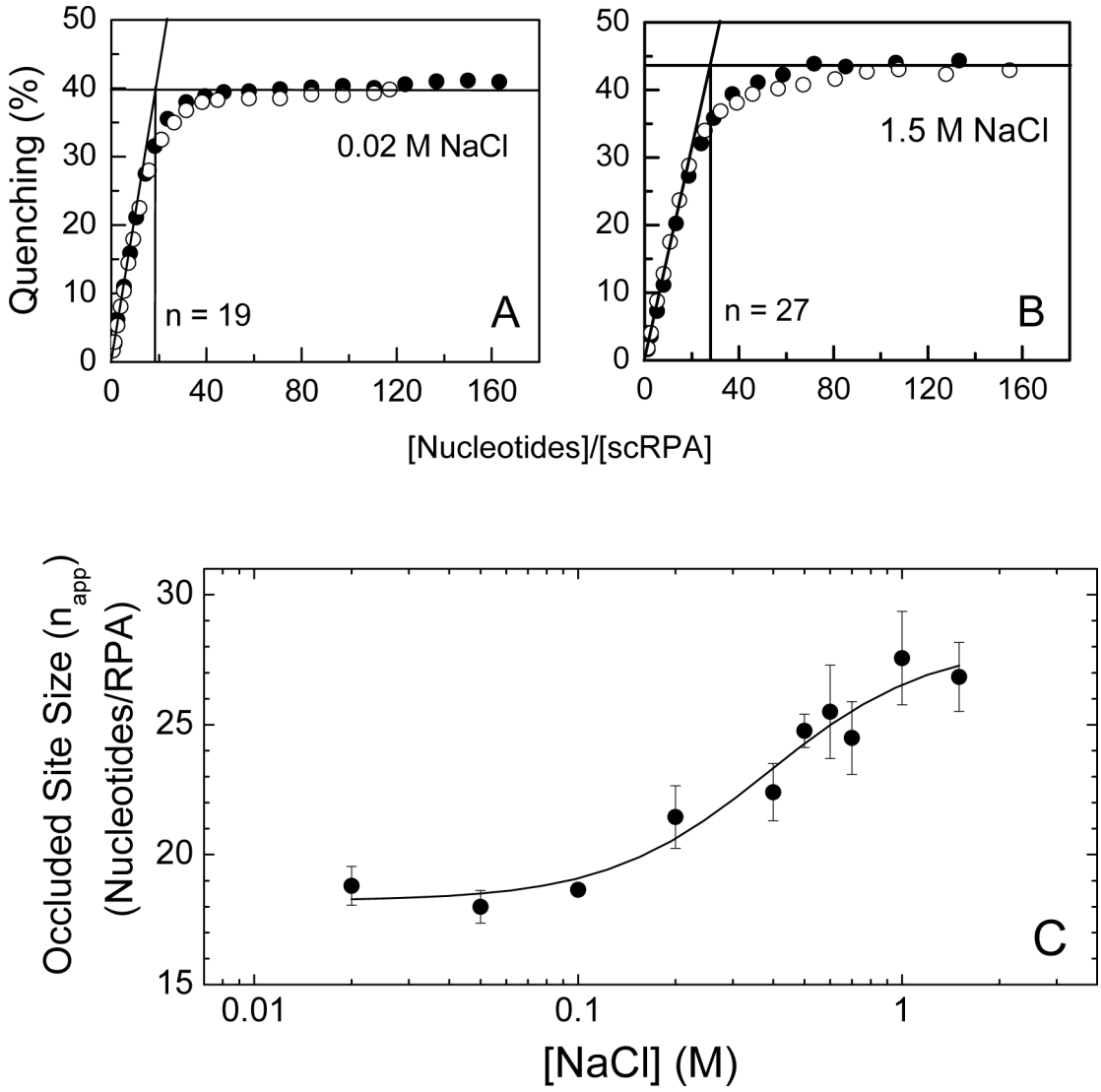

Figure 3. Salt dependence of occluded site size for scRPA binding to poly(dT)

Results of titrations of scRPA with poly(dT) (buffer T, pH 8.1, 25°C) monitoring the quenching of scRPA tryptophan fluorescence (λ_{excit}= 295 nm and λ_{emis} =345 nm) at (A) 20 mM NaCl, and (B) 1.5 M NaCl. Each panel shows the results of two titrations obtained at two scRPA concentrations: (●) - 0.1 μM, and (○) - 0.2 μM. The occluded site size (n_{app}) was determined from the intersection of the two lines as indicated and is 19 ± 1 nucleotides at 20 mM NaCl and 27 ± 2 nucleotides at 1.5 M NaCl. (C) – The occluded site size (n_{app}) for scRPA binding to poly(dT) plotted as a function of [NaCl] (buffer T, pH 8.1, 25.0 °C). The solid line simulates the transition between a low salt binding mode with *n* = (18 ± 1) nucleotides and a high salt binding mode with *n* = (27 ± 2) nucleotides with a transition at ~ 0.36 M NaCl.

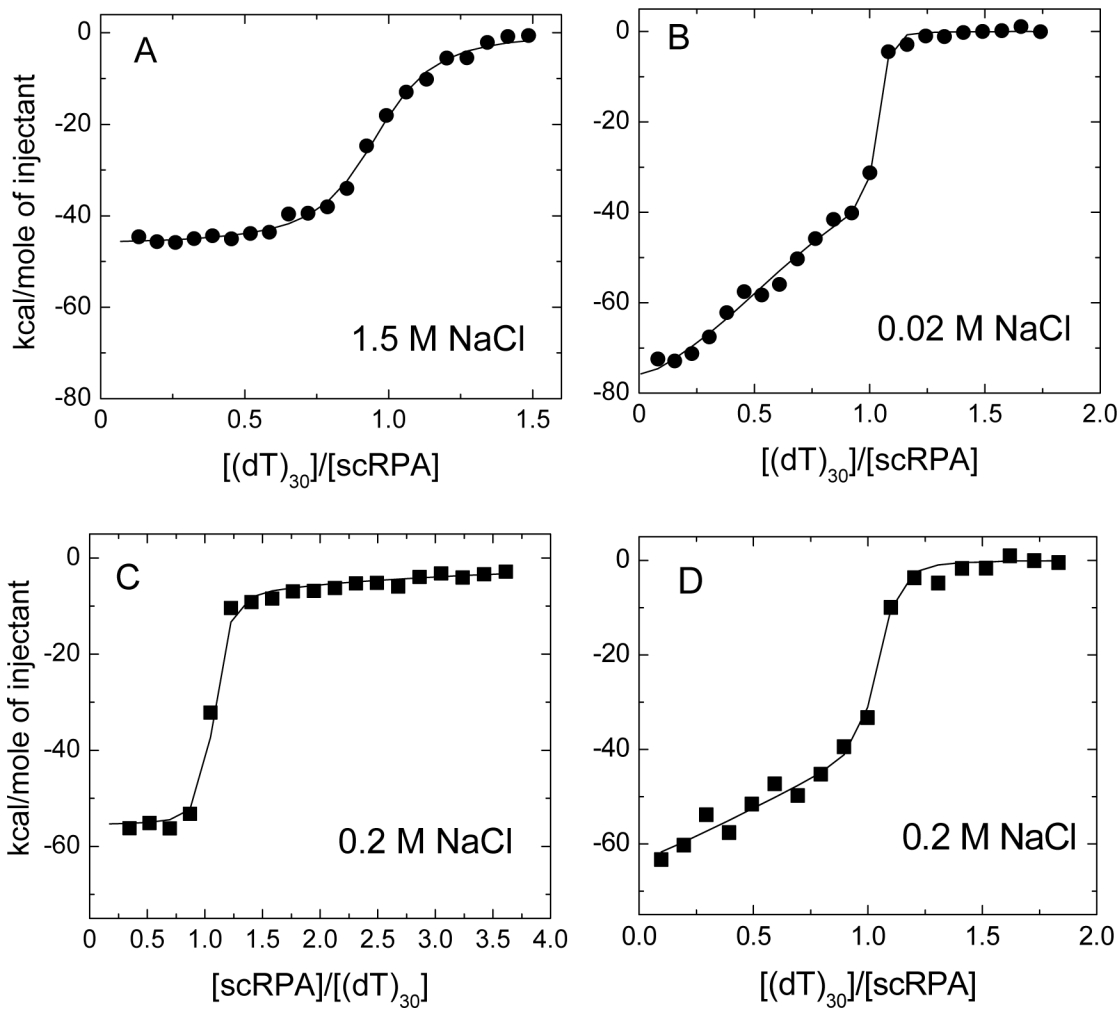

Figure 4. Stoichiometry of scRPA binding to $(dT)_{30}$ is influenced by [NaCl]

Results of ITC titrations of scRPA with $(dT)_{30}$, plotted as normalized heat per mole of injectant, (panels A, B and D) and of $(dT)_{30}$ with scRPA (panel C). (A) - titration of scRPA (0.72 μM) with $(dT)_{30}$ (6.4 μM) at 1.5 M NaCl (buffer T, pH 8.1, 25°C). The solid line represents the best fit of the data to a single site binding model (eq 7) yielding: $K=(1.21\pm0.14)\times10^8\ M^{-1}$ and $\Delta H_{obs} = -46.2\pm0.5$ kcal/mol. (B) - titration of scRPA (0.6 μM) with $(dT)_{30}$ (6.2 μM) at 20 mM NaCl (buffer T, pH 8.1, 25°C). The solid line represents the best fit to a two site binding model (eq 8), yielding: $K_1=(1.6\pm0.8)\times10^{10}\ M^{-1}$; $\Delta H_1=-56.5\pm0.5$ kcal/mol and $K_2=(2.4\pm1.5)\times10^6\ M^{-1}$; $\Delta H_2=-32.7\pm10.0$ kcal/mol. (C) - titration of $(dT)_{30}$ (0.43 μM) with scRPA (15.1 μM) at 0.20 M NaCl (buffer T, pH 8.1, 10% (v/v) glycerol, 25°C). The solid line represents the best fit to a two site binding model (eq 8), yielding: $K_1=(9.3\pm5.6)\times10^8\ M^{-1}$; $\Delta H_1=-55.4\pm1.1$ kcal/mol and $K_2=(6.0\pm5.2)\times10^5\ M^{-1}$; $\Delta H_2=-37.1\pm19.0$ kcal/mol. (D) - titration of scRPA (1.1 μM) with $(dT)_{30}$ (21.1 μM) performed in the same buffer condition as in (C). The solid line represents the best fit to a two site binding model (eq 8) yielding: $K_1=(8.9\pm4.5)\times10^8\ M^{-1}$; $\Delta H_1=-51.6\pm1.0$ kcal/mol and $K_2=(5.3\pm5.5)\times10^5\ M^{-1}$; $\Delta H_2=-30.2\pm22.0$ kcal/mol.

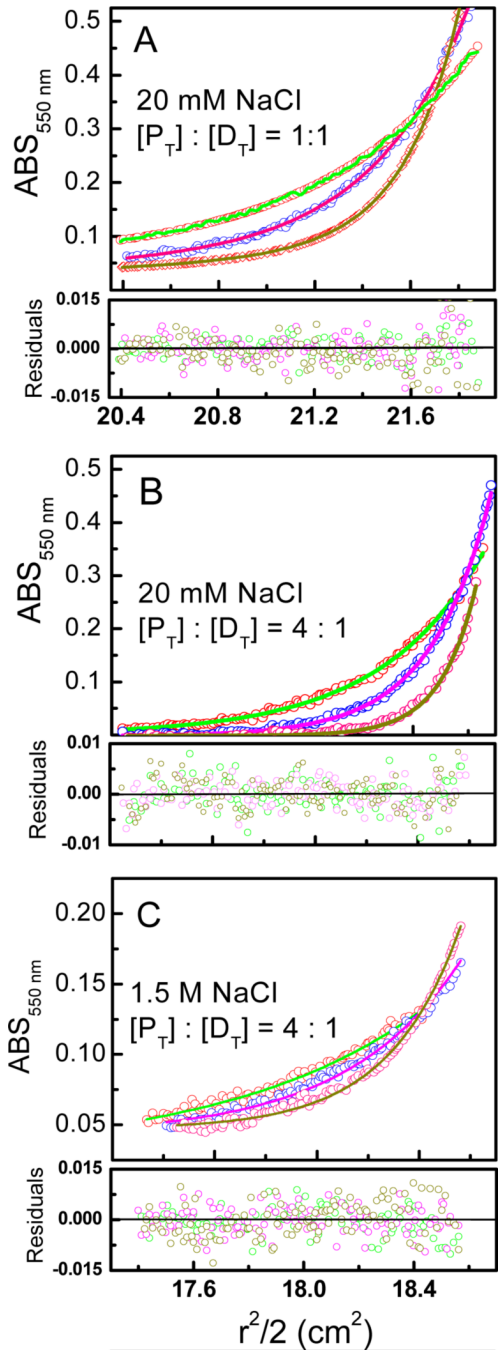

Figure 5. Stoichiometries of scRPA-5′Cy3-$(dT)_{29}$ complexes examined by sedimentation equilibrium

(A) – Results of experiments performed at a 1:1 molar ratio of scRPA (1.27 μM) to 5′Cy3-$(dT)_{29}$ (1.27 μM) at 20 mM NaCl (buffer T, pH 8.1, 25°C) at three rotor speeds 10 krpm (green), 13 krpm (magenta), 17 krpm (dark yellow). These data fit well to a single species model (eq 1), yielding a molecular mass, M = 113± 1 kDa, which is close to that expected for a 1:1 complex (123 kDa). (B) – Results of experiments performed at a four-fold molar excess of scRPA (2.4 μM) over 5′Cy3-$(dT)_{29}$ (0.6 μM) at 20 mM NaCl (buffer T, pH 8.1, 25°C) at three rotor speeds 10 krpm (green), 13 krpm (magenta), 17 krpm (dark yellow). The data fit well to a single species model (eq 1) yielding a weight average molecular mass, M = 222.8 ± 2.0 kDa,

close to the expected value of 218 kDa for a complex of two scRPA bound to one 5′Cy3-$(dT)_{29}$. (C) – Results of experiments performed at a four fold molar excess of scRPA (2.4 μM) over 5′Cy3-$(dT)_{29}$ (0.6μM) in 1.5 M NaCl (buffer T, pH 8.1, 25°C) at three rotor speeds 10 krpm (green), 13 krpm (magenta), 17 krpm (dark yellow). The data fit well to a single species model (eq 1) yielding a molecular mass, M = 127± 3 kDa, which is close to that expected for a 1:1 complex (123 kDa).

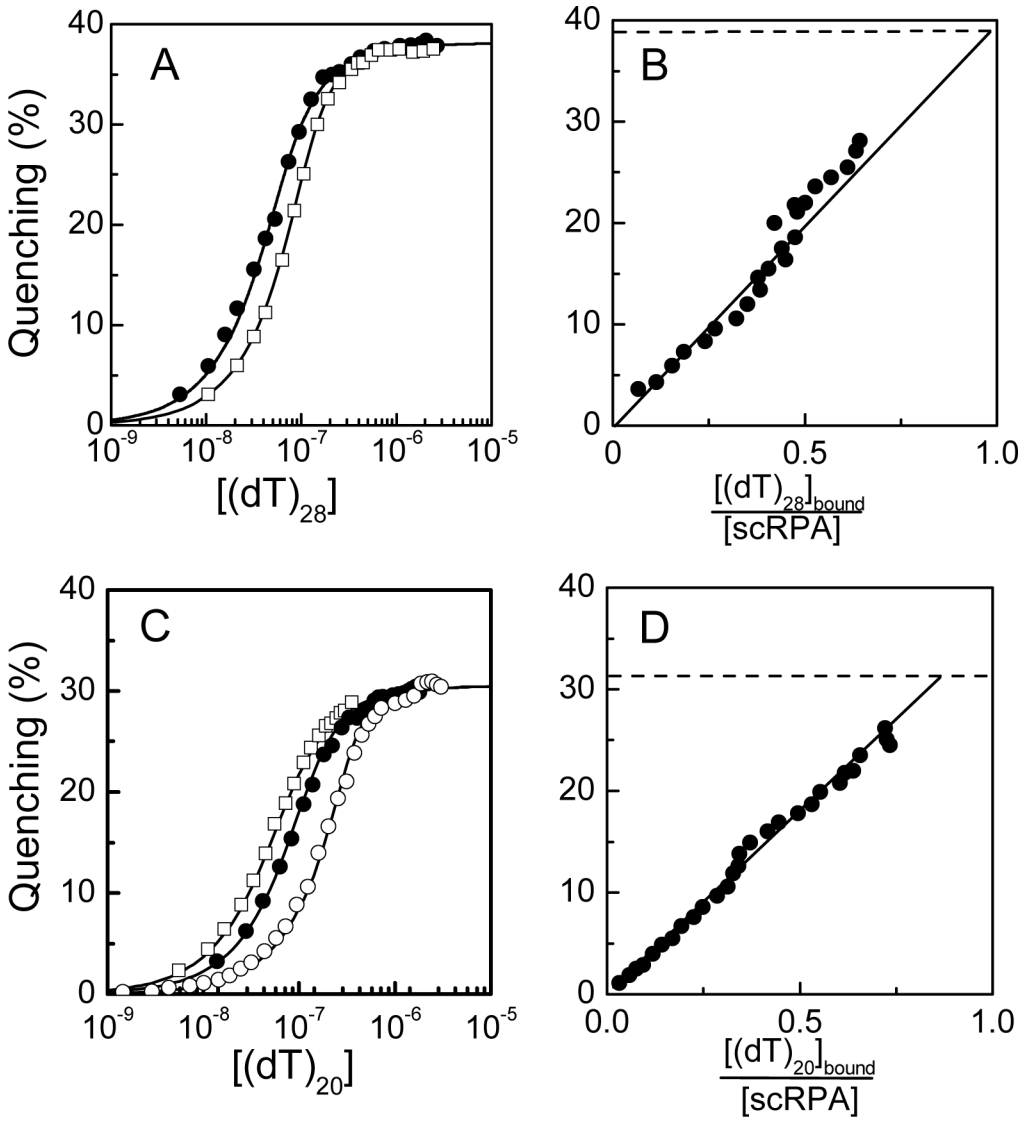

Figure 6. Fluorescence Binding isotherms show that 1:1 complexes of scRPA with $(dT)_{28}$ and $(dT)_{20}$ are formed at 1.5 M NaCl

(A)- Results of equilibrium fluorescence titrations of scRPA with $(dT)_{28}$ at two scRPA concentrations: (●) 6.0×10^{-8} M; (□) 1.2×10^{-7} M (buffer T, pH 8.1, 25°C, 1.5 M NaCl), monitoring the quenching of the scRPA tryptophan fluorescence. Global fitting of the two titrations to a single site binding model (eq 5) yields $K_{obs} = 6.72 \pm 0.42 \times 10^7$ M^{-1}, and $Q_{max} = 0.38 \pm 0.01$. The solid lines are simulations based on eq 5 and the best fit parameters. (B)- Analysis of the data in panel (A) using the model-independent binding density function method shows that the fluorescence quenching of scRPA is directly proportional to the average number of $(dT)_{28}$ bound per scRPA heterotrimer. Linear extrapolation of the data to the known maximum fluorescence quenching at saturation yields a stoichiometry of 1.0 $(dT)_{28}$/scRPA. (C)- Results of equilibrium fluorescence titrations of scRPA with $(dT)_{20}$ at three scRPA concentrations: (□) 3.0×10^{-7} M (●), 1.0×10^{-7} M; (○) 0.5×10^{-7} M (buffer T, pH 8.1, 25° C, 1.5 M NaCl). Global fitting of the two titrations to a single site binding model (eq 5) yields $K_{obs} = 4.02 \pm 0.21 \times 10^7$ M^{-1}, and $Q_{max} = 0.31 \pm 0.01$. The solid lines are simulations based on eq 5 and the best fit parameters. (D) - Dependence of scRPA fluorescence quenching on the average number of $(dT)_{20}$ bound per scRPA, obtained from analysis of the data in panel (C)

using the binding density function method. The solid line shows a linear extrapolation of the data to the known maximum fluorescence quenching at saturation yields a stoichiometry of 1.0 $(dT)_{20}$/scRPA.

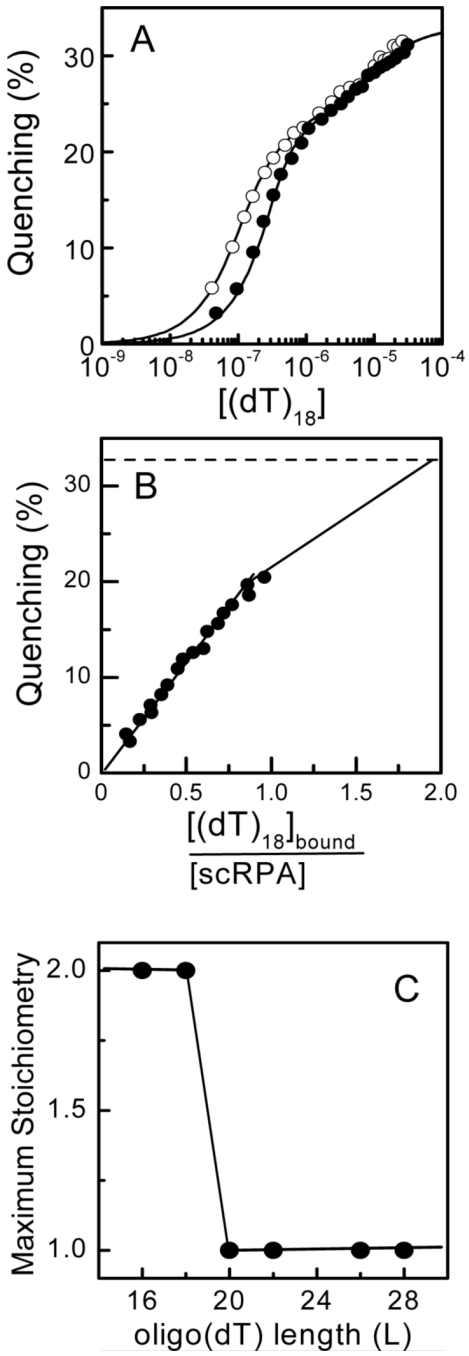

Figure 7. Equilibrium binding isotherms show that two molecules of $(dT)_{18}$ can bind per scRPA at high salt

(A) – Equilibrium titrations monitoring the scRPA tryptophan fluorescence quenching upon binding $(dT)_{18}$ obtained at two scRPA concentrations: (○)1.0×10^{-7} M (●) 3.6×10^{-7} M at 1.5 M NaCl (buffer T, pH 8.1, 25°C). The continuous lines represent simulations based on a model for two molecules of $(dT)_{18}$ binding per scRPA (eq 6). A global NLLS fit of both titrations yields $K_{1,obs} = 2.08 \pm 0.22 \times 10^7$ M^{-1} and $K_{2,obs} = 1.29 \pm 0.26 \times 10^5$ M^{-1} for the macroscopic binding constants for binding of the first and the second $(dT)_{18}$ to scRPA. (B) - Dependence of relative tryptophan fluorescence quenching of scRPA on the average number of $(dT)_{18}$ molecules bound per scRPA obtained from analysis of the titrations in panel (A).

The relationship for the second phase of the titrations could not be obtained due to the weak binding affinity. However, a linear extrapolation from the points at $[(dT)_{18}]/[scRPA] = 1$ to the known maximum fluorescence quenching at saturation ($Q_{max} = 0.33 \pm 0.01$) yields a maximum stoichiometrry of 2 moles of $(dT)_{18}$ bound per scRPA. (C) - Dependence of the maximum stoichiometry (maximum number of $(dT)_L$ molecules that can bind per scRPA) as a function of the ss-oligodeoxythymidylate length, L (1.5 NaCl, buffer T, pH 8.1, 25° C), showing a clear transition between L = 18 and 20 nucleotides.

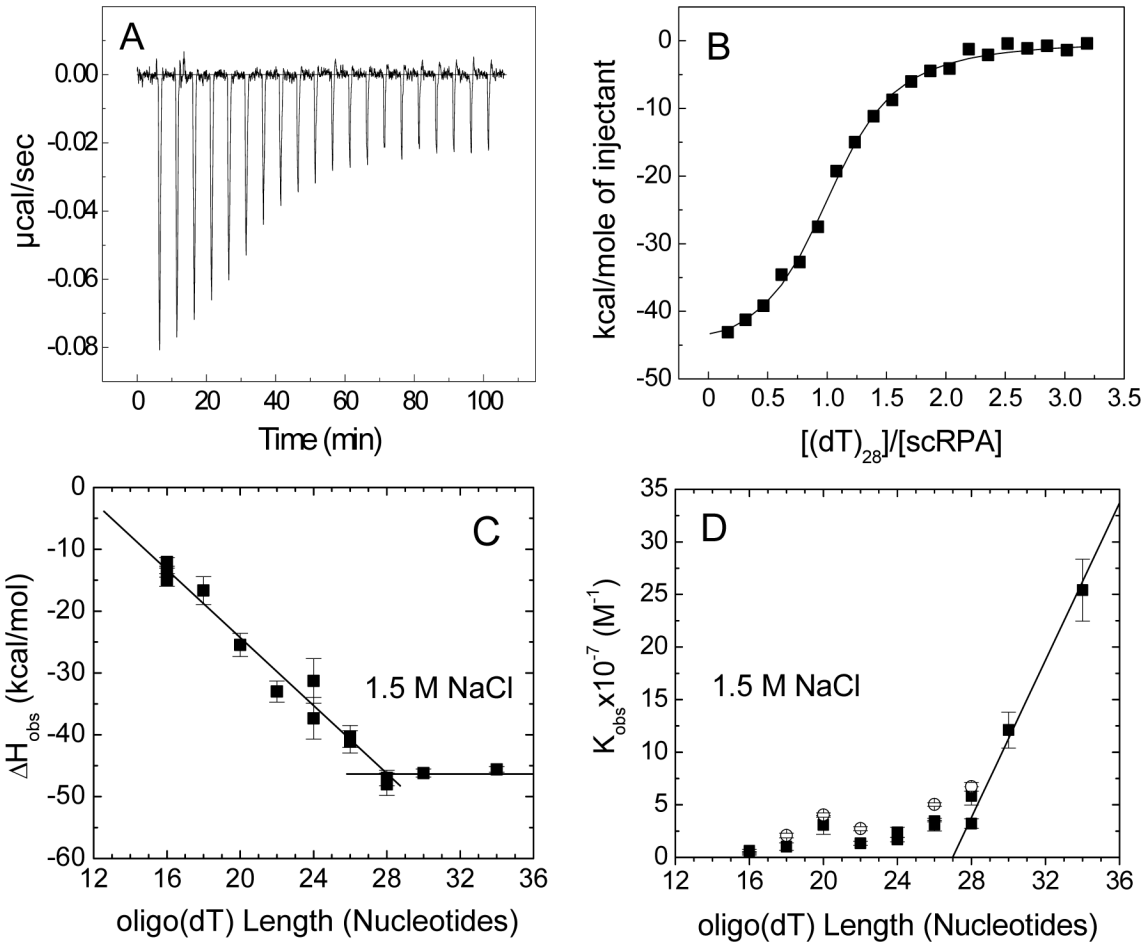

Figure 8. Determination of the scRPA contact size at 1.5 M NaCl

(A) – Results of an ITC titration of scRPA (0.24 μM in the cell) with $(dT)_{28}$ (5.0 μM in the syringe) (buffer T, pH 8.1, 1.5 M NaCl, 25°C). (B) - integrated heat responses from data in (A) are plotted as injection heats (kcal) per mole of injected DNA. The smooth line represents the best fit to a 1:1 binding model (eq 7) with parameters $K_{obs} = 4.8 \times 10^7 \pm 0.5$ and ΔH_{obs}= −47±1 kcal/mol. (C) - Dependence of ΔH_{obs} on ssDNA length, *L*, determined for scRPA binding to a series of oligodeoxynucleotides, $(dT)_L$ (buffer T, pH 8.1, 1.5 M NaCl, 25°C). A contact size of *m*=28 nucleotides is estimated from the intercept of the line describing the linear dependence of ΔH_{obs} on *L*, with the plateau value of $\Delta H_{obs} = -46 \pm 2$ kcal/mol at $L \geq 30$. (D) - Dependence of the observed equilibrium binding constant, K_{obs}, on ss-oligodeoxynucleotide length, *L*. (■) - data from ITC titrations, (○) - data from fluorescence titrations. A contact size of *m*=27−28 nucleotides is determined from the intercept of a linear extrapolation of the data for $L \geq 28$ nucleotides to $K_{obs} = 0$.

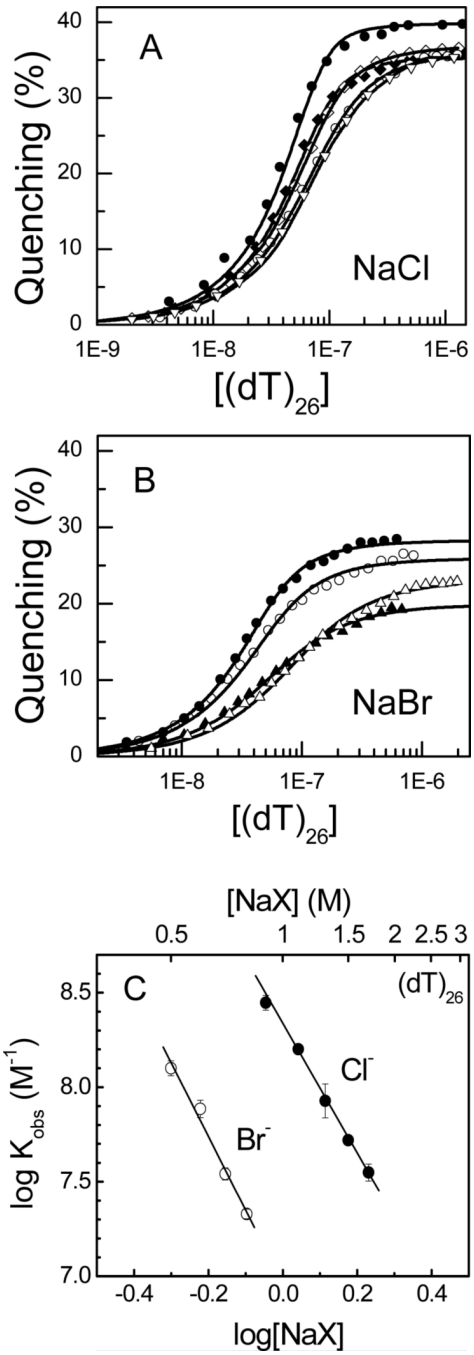

Figure 9.

Dependence on NaCl and NaBr concentrations of the equilibrium constant for scRPA binding to $(dT)_{26}$. Equilibrium binding was monitored by the quenching of scRPA (50−90 nM) tryptophan fluorescence upon binding $(dT)_{26}$ (buffer T, pH 8.1, 25°C). (A) - Binding isotherms obtained as a function of [NaCl]: 0.90 M (●); 1.10 M (◆); 1.30 M (◇); 1.50 M (○) and 1.70 M (▽). Solid lines represent best fits of the data to a single site binding model (eq 5). (B) - Binding isotherms obtained as a function of [NaBr]: 0.50 M (●); 0.60 M (○); 0.70 M (△), and 0.80 M (▲).Solid lines represent best fits of the data to a single site binding model (eq 5). (C) - Dependence of K_{obs} (obtained from analysis of the data in panels A and B) on salt

concentration (log-log plots); $\partial \log K/\partial \log[NaCl] = -3.42 \pm 0.07$, and $\partial \log K/\partial[NaBr] = -3.87 \pm 0.15$.

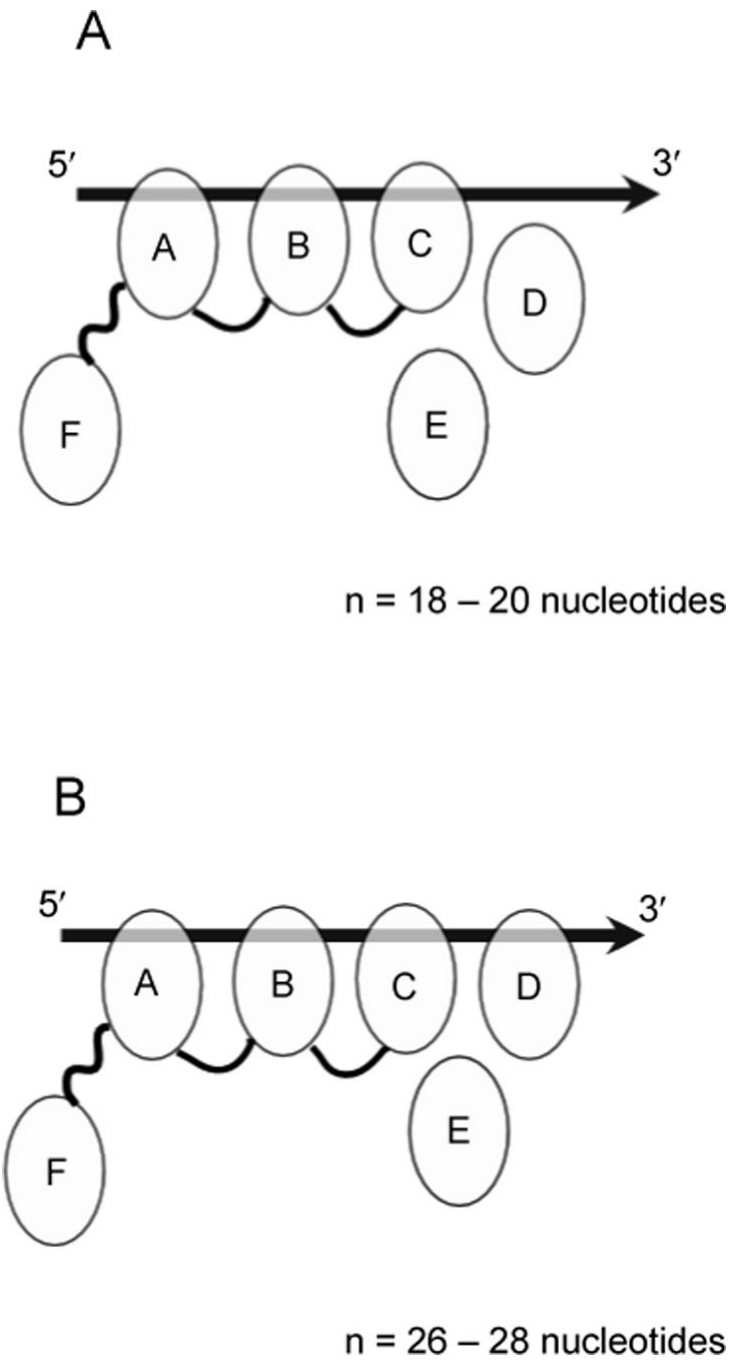

Figure 10.

Schematic representation showing that the two scRPA modes of binding to long ssDNA differ in the number of OB-folds that interact with the ssDNA. (A) - low salt binding mode in which scRPA uses only three of its OB-folds (A, B, C) contained within the RPA70 subunit to bind ssDNA with an occluded site size of 18−20 nucleotides. (B) - high salt binding mode in which scRPA uses the three OB-folds within the RPA70 subunit plus an additional OB-fold (D) from the RPA32 subunit to bind ssDNA with an occluded site size of 26−28 nucleotides.

Table 1

Molecular mass determined for scRPA by sedimentation equilibrium experiments at 25 °C.

Buffer Conditions	Expected Molecular Mass (kDa)	Observed Molecular Mass (kDa)
Buffer T + 20 mM NaCl	114	115 ± 5
Buffer T + 1.0 M NaCl	114	119 ± 3
Buffer T + 1.5 M NaCl	114	122 ± 4
Buffer T + 0.2 M NaCl + 10% Glycerol	114	118 ± 3

Table 2

Occluded site size (n) of scRPA binding to poly(dT) under different buffer conditions. Conditions: 10 mM Tris, pH 8.1, 0.1 mM Na_3EDTA, 25.0 °C

[NaCl] (M)	[$MgCl_2$] (mM)	Site size (Nucleotide/scRPA
0.02		19 ± 1
0.05		18 ± 1
0.1		19 ± 1
0.2		21 ± 1
0.4		22 ± 1
0.5		25 ± 1
0.6		26 ± 1
0.7		25 ± 1
1.0		28 ± 2
1.5		27 ± 2
	1.0	20 ± 1
	5.0	20 ± 1
	10.0	22 ± 1

Table 3

Thermodynamic and spectroscopic properties for the binding of ssDNA oligomers to scRPA in buffer T, 1.5 M NaCl, at 25°C.

$(dT)_L$ (Length)	Absolute Stoichiometry	$K_{1,obs}\times10^{-7}$ (M^{-1})	$K_{2,obs}\times10^{-5}$ (M^{-1})	$\Delta F_{1,obs}$	$\Delta F_{2,obs}$	$\Delta F_{max,obs}$
18	2	2.1 ± 0.2	1.3 ± 0.3	0.23±0.01	0.10±0.01	0.33 ± 0.01
20	1	4.0 ± 0.2				0.31 ± 0.01
22	1	2.7 ± 0.2				0.32 ± 0.01
26	1	5.0 ± 0.2				0.33 ± 0.01
28	1	6.7 ± 0.4				0.38 ± 0.01